

# Magnetic Materials and Devices for the 21st Century: Stronger, Lighter, and More Energy Efficient

Oliver Gutfleisch,\* Matthew A. Willard, Ekkes Brück, Christina H. Chen, S. G. Sankar, and J. Ping Liu

A new energy paradigm, consisting of greater reliance on renewable energy sources and increased concern for energy efficiency in the total energy life-cycle, has accelerated research into energy-related technologies. Due to their ubiquity, magnetic materials play an important role in improving the efficiency and performance of devices in electric power generation, conditioning, conversion, transportation, and other energy-use sectors of the economy. This review focuses on the state-of-the-art hard and soft magnets and magnetocaloric materials, with an emphasis on their optimization for energy applications. Specifically, the impact of hard magnets on electric motor and transportation technologies, of soft magnetic materials on electricity generation and conversion technologies, and of magnetocaloric materials for refrigeration technologies, are discussed. The synthesis, characterization, and property evaluation of the materials, with an emphasis on structure–property relationships, are discussed in the context of their respective markets, as well as their potential impact on energy efficiency. Finally, considering future bottlenecks in raw materials, options for the recycling of rare-earth intermetallics for hard magnets will be discussed.

Dr. O. Gutfleisch  
Institute of Metallic Materials  
IFW Dresden, 01069 Dresden, Germany  
E-mail: o.gutfleisch@ifw-dresden.de

Dr. M. A. Willard  
Naval Research Laboratory  
Code 6355, 4555 Overlook Ave., S. W.  
Washington, DC 20375 – 5343, USA

Prof. E. Brück  
Faculty of Applied Sciences  
Delft University of Technology  
2629 JB Delft, The Netherlands

Dr. C. H. Chen  
Magnetics Laboratory  
University of Dayton  
Dayton, OH 45469, USA

Dr. S. G. Sankar  
Advanced Materials Corporation  
850 Poplar Street, Pittsburgh, PA 15220, USA

Prof. J. P. Liu  
Department of Physics  
University of Texas at Arlington  
Arlington, TX 76019, USA

DOI: 10.1002/adma.201002180

## 1. Energy Consumption and the Need for High-Efficiency Devices

Human development has caused a depletion of natural energy resources and climate changes with unpredictable consequences. New energy concepts are required for the future of our industrial society, resulting in an ever-increasing emphasis on improving the efficiency of electricity transmission and utilization and in the progressive replacement of oil-based fuels in transportation by electric motors. In this context, functional magnetic materials, such as advanced hard and soft magnets, magnetic refrigerants, magnetic MEMS (microelectromechanical systems), magnetic shape memory alloys, and magnetorheological fluids and elastomers, can have a substantial impact on improving these technologies. This review will show that magnetic materials are essential components of energy applications (i.e., motors,

generators, transformers, actuators, etc.) and improvement in magnetic materials will have significant impact in this area, on par with many “hot” energy materials efforts (e.g., hydrogen storage, batteries, thermoelectrics, etc.). This section will highlight some technology sectors where magnetic materials have a clear impact, including transportation, electric power generation and conversion, and refrigeration.

Electric motors have been ubiquitous in driving the technological society for the past couple of centuries. Motors ranging from a few watts to several hundred kilowatts have been widely employed in office and household appliances, the transportation sector, and industrial drives. In developed countries such as the USA, nearly 30% of this electricity is consumed by the industrial sector and, of that, nearly 65% is consumed by electric motor drives.<sup>[1]</sup> Thus the consumption of electricity energy by motors, both big and small, in the USA alone, accounts for nearly 750 billion kWh or, at an average price of \$0.06 per kWh, nearly 45 billion US dollars. A 1% improvement in efficiency would result in the savings of hundreds of millions of dollars and a reduction in CO<sub>2</sub> emissions of nearly 2.2 million metric tons of carbon equivalent. Even a small improvement in energy efficiency for electric motors can have a large economical and environmental savings. This is where permanent magnets and

**Table 1.** World Total Net Electricity Consumers. Reproduced from.<sup>[2]</sup>

| Country                        | Electricity Consumed (Trillion kWh) |
|--------------------------------|-------------------------------------|
| USA                            | 3.82                                |
| European Union                 | 2.93                                |
| China                          | 2.53                                |
| Japan                          | 0.98                                |
| Russia                         | 0.82                                |
| Canada                         | 0.53                                |
| India                          | 0.52                                |
| Other Countries                | 4.25                                |
| <b>Total World Consumption</b> | <b>16.38</b>                        |

soft magnets play a major role by providing a smaller, lighter weight electric motor with the necessary power and torque required for transportation and actuation applications.

Electricity consumed by the entire world population is estimated to be about 16.38 trillion kWh (2006 estimates) broken down by region, as shown in **Table 1**.<sup>[2]</sup> People in the USA consumed 4.2 trillion kWh of electricity in 2007, a number that is expected to grow from today's 33% of our total energy consumption to 50% by 2015.<sup>[3]</sup> Modern lighting, consumer electronics, and transportation consistently require higher levels of power quality and more total electrical power. This is irrespective of an increase in the green energy sectors of electric power generation (see **Figure 1** (left)). The need for efficient generation, transmission, and distribution of electric power is ever growing, however, the trend in efficiency has shown an alarming development (**Figure 1** (right)), with annual electric losses outpacing annual increases in electricity consumption by a factor of more than two-to-one (49.4 and 23.4 TW per yr, respectively). As a result, while more energy can be produced from renewable sources, electrical losses must also be addressed.

With the anticipated increase in demand for electric transportation (including hybrid and electric vehicles, HEVs and EVs), the consumption of electricity will increase significantly above its current 2.5% annual increase. Therefore, it is necessary to offset at least a part of the increased consumption of electricity through innovative design and development of high-efficiency motors, generators, and power converters. However, improving the efficiency of the existing infrastructure will not be enough to address the increased demand for electricity, which has driven the acceleration of research and development



**Oliver Gutfleisch** graduated in 1991 in Materials Science at the Technical University of Berlin, Germany. In 1995 he earned his Ph.D. at the School of Metallurgy and Materials, University of Birmingham, UK, and continued his work there on rare-earth transition metal compounds for permanent magnet applications as a research fellow. He joined the Leibniz Institute of Solid State and Materials Research (IFW Dresden, Germany) in 1998, leading a research group on functional materials for sustainable energy. In 2007 he earned his habilitation at the Technical University of Dresden. He currently is a visiting professor at the Imperial College London and a visiting advisor at NIMS Tsukuba, Japan. In 2011 he is a Distinguished Lecturer of the IEEE Magnetics Society for "Magnetic Materials in Sustainable Energy".

of clean and renewable energy sources. Renewable or sustainable energy refers to the conversion of solar, wind, ocean, hydro-power, biomass, and geothermal energy into electric power.

The largest electric consumptions for the residential market in the USA are refrigeration for food and air conditioning, which contribute over 25% of the total for the average household. Conventional cooling methodologies using vapor-compression refrigerators prove to be bulky, heavy, and energy inefficient. Recently, the use of the adiabatic demagnetization (the so-called magnetocaloric effect (MCE)) for room-temperature refrigeration was demonstrated to have ≈30% better energy efficiency than competing vapor-compression refrigeration techniques, without the environmentally detrimental refrigerant gases.<sup>[5]</sup> Advances in MCE materials will enable solid-state technologies to improve refrigeration capacities and efficiencies.

Whether referred to as sustainable, renewable, or alternative energy, a large number of new sources for the generation of electricity are likely to be added to the grid in the next decade.<sup>[6,7]</sup> This will require a strong investment in energy efficient methods for power generation. In some cases, such as wind power and transportation, improvements demand not only higher efficiency but also smaller size and weight of the

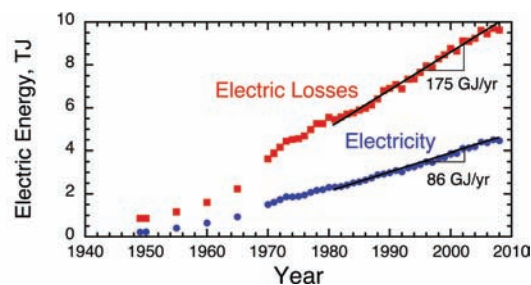
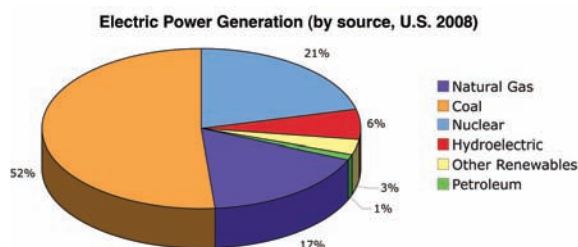


**Figure 1.** (left) Electric power generation in the United States by source for 2007. (right) Residential electricity consumption since 1949. Electric losses include energy lost from generation, transmission, and distribution. Data from Ref. [4].

materials and devices. Equally important to sustainable investment in electricity sustainability is developing higher energy efficiency for power conversion. Advanced permanent and soft magnet materials provide high efficiency and reliability and compact, low cost, and low maintenance solutions for renewable energy technologies, including wind turbines, hydroelectric power generators, and wave power buoys.

## 2. Hard Magnetic Materials

During the twentieth century, several permanent magnet materials were discovered. Techniques to effectively manufacture these magnets have been established.<sup>[8]</sup> Device designs using such magnets in various active and passive applications have been successfully exploited. The energy product, which is a key figure of merit of permanent magnets, has been enhanced, starting from  $\approx 1$  MGOe for steels discovered during the early part of the century, increasing to  $\approx 3$  MGOe for hexagonal ferrites, and finally peaking at  $\approx 56$  MGOe for neodymium-iron-boron magnets during the past ten years. With this, almost 90% of the limit for the energy density,  $(BH)_{\max}$ , (based on the  $\text{Nd}_2\text{Fe}_{14}\text{B}$  phase) can be achieved in commercially produced sintered Nd-Fe-B grades. The historical evolution, spanning nearly 100 years, of these permanent magnets is shown in **Figure 2**. At the time of writing, however, it appears that the search for novel hard magnetic compounds with higher remanent magnetization, defined now as the relevant parameter, has somewhat stagnated and no further breakthrough is in sight. On the other hand, only a small number of ternary and quaternary systems have been investigated so far. The approach of nanocomposites is the one that is currently the most actively pursued, with particular emphasis on attempting to have the hard magnetic phase textured, as well as exchange-coupled with a soft magnetic phase; the latter phase has an intrinsic upper limit of

$\mu_0 M_s = 2.43$  T for an  $\text{Fe}_{65}\text{Co}_{35}$  alloy, where  $\mu_0$  is the permeability of free space and  $M_s$  is the saturation magnetization.

Recently, there is a much revived interest in various types of high-performance permanent magnets based on rare-earth intermetallic compounds. This is triggered by, for example, the growing demand for energy efficient technologies in which these magnets often play a pivotal part. Generally, the major driving force for research and development of rare-earth permanent magnets (RPMs) is the need for maximized energy densities at various operating temperatures. Most importantly, this includes less Dy-containing  $\text{Nd}_2\text{Fe}_{14}\text{B}$ -type magnets with much improved temperature stability for electromotor applications at around 450 K,<sup>[9]</sup>  $\text{Pr}_2\text{Fe}_{14}\text{B}$ -type magnets for applications at 77 K together with high Curie temperature ( $T_c$ ) superconductors,<sup>[10]</sup> and a new generation of SmCo 2:17-type magnets for applications at temperatures exceeding 670 K.<sup>[11,12]</sup> It also includes magnetic-power MEMS,<sup>[13–16]</sup> for example, a high-speed permanent magnetic generator, which require highly textured, thick RPM films.<sup>[17]</sup> Nowadays, emphasis of research is on the control of microchemistry and structure of grain boundary phases and internal interfaces, which are crucial for the understanding of the relevant coercivity mechanisms and the related critical elementary magnetization reversal processes. Textured nanocomposites could be the next generation of permanent magnets. This would involve mastering the fabrication of intimately mixed multiphase and well-oriented nanoscale magnets, which cannot be done by conventional processing techniques.

### 2.1. General Considerations for Permanent Magnetic Materials in Energy Applications

Permanent magnetic materials used in electric machines perform one basic function, which is to provide magnetic flux. This function requires a saturation magnetization ( $4\pi M_s$  in cgs units or  $J_s = \mu_0 M_s$  in SI units) as high as possible and affordable, as well as an appropriate coercivity. **Figure 3** shows the saturation magnetization versus intrinsic coercivity,  $iH_c$  for major soft and hard magnetic materials. Most of the soft magnetic materials have  $iH_c \ll 1$  kA  $\text{m}^{-1}$  and the hard magnetic materials have  $iH_c$  up to  $\approx 2800$  kA  $\text{m}^{-1}$  ( $\approx 35$  kOe).

For permanent magnets, coercivity is the ability to resist demagnetization, including field demagnetization from the electric or magnetic circuit and thermal demagnetization from the operating temperature. Coercivity is extremely important for motor applications since these two demagnetization actions occur continuously while motors are running. Two coercivity parameters are used to grade the magnetic hardness: one is intrinsic coercivity,  $iH_c$  (or  $jH_c$ ), and the other is normal (or technical) coercivity,  $H_c$ . The permanent magnets suitable for such applications must have high coercivity and ideally  $iH_c$  is much higher than  $H_c$ , which allows the magnets to have linear demagnetization induction ( $B$ ) curve in the second quadrant. Linear  $B$  curve is a very important characteristic that enables the magnets to be stable during operation. Only three types of permanent magnets shown in **Figure 3** possess such capability: these are hard ferrites, Nd-Fe-B, and Sm-Co magnets. Four pairs of demagnetization curves at room temperature are shown in **Figure 4** for those three magnets and for an Alnico magnet. As

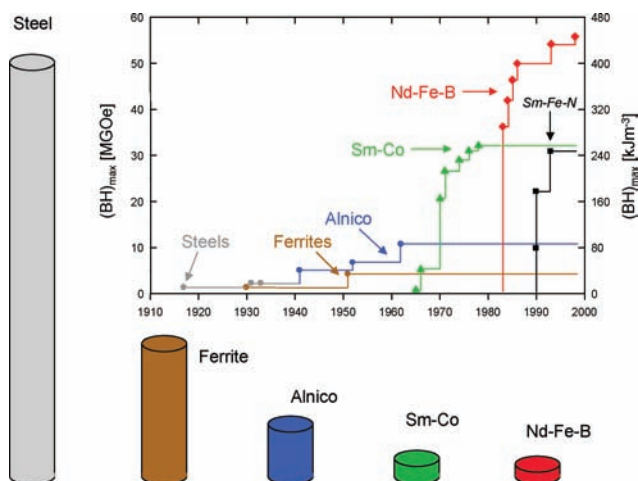


**Figure 2.** Development in the energy density  $(BH)_{\max}$  at room temperature of hard magnetic materials in the 20th century and presentation of different types of materials with comparable energy density (each magnet is designed so that at a reference point 5 mm from the surface of the pole, a field of 100 mT is produced).

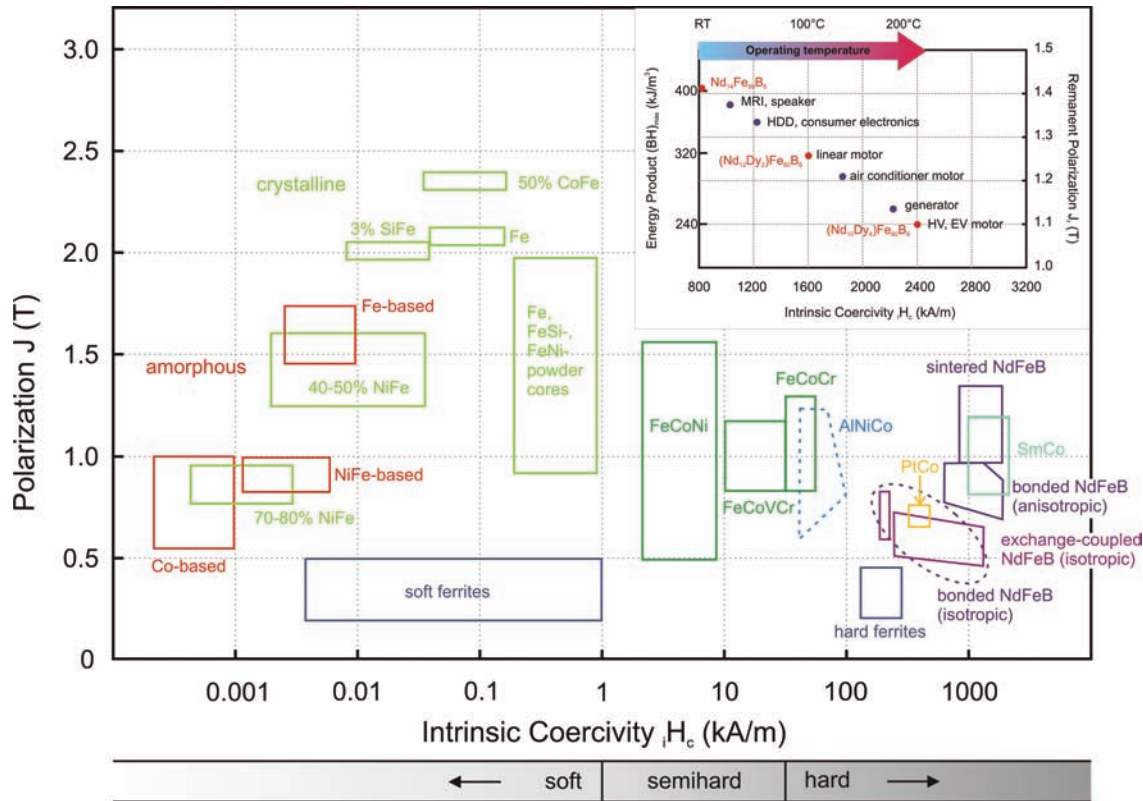


**Figure 3.** Polarization versus coercivity of soft and hard magnetic materials. The inset shows a closer look at high energy density NdFeB-type magnets with various Dy-contents for applications from room temperature to 200 °C.

shown in Figure 4, Alnico has nonlinear demagnetization curves and it is not suitable for motor applications. Sm-Co type magnets have a very good, linear  $B$  curve at room temperature and retain the linear  $B$  curve in the temperature range of 300 °C to 550 °C, depending on the alloy composition.<sup>[11,12,18,19]</sup> Nd-Fe-B, plotted in Figure 4(left), is not a good candidate for motor applications since a nonlinear  $B$ - $H$  curve with a “knee” is shown on its  $B$  curve, which indicates instability of this magnet when it is surrounded in the electric field at elevated temperature. High

coercivity  $(\text{Nd}_{10}\text{Dy}_4)\text{Fe}_{80}\text{B}_6$  magnets with 4 at% Dy substitution for Nd were developed for such applications. As shown in Figure 4(right), the Dy added Nd-Fe-B retains linear  $B$  curves at temperatures up to about 175 °C. Most of commercially available hard ferrites do not have a linear  $B$  curve at room temperature; however, that does not prevent ferrite from being used for motor applications since ferrite has a unique positive temperature coefficient of coercivity, as shown in Figure 5.<sup>[20]</sup> The  $iH_c$  of the ferrite magnet increases from 3.2 kOe at 0 °C to 5.9 kOe at

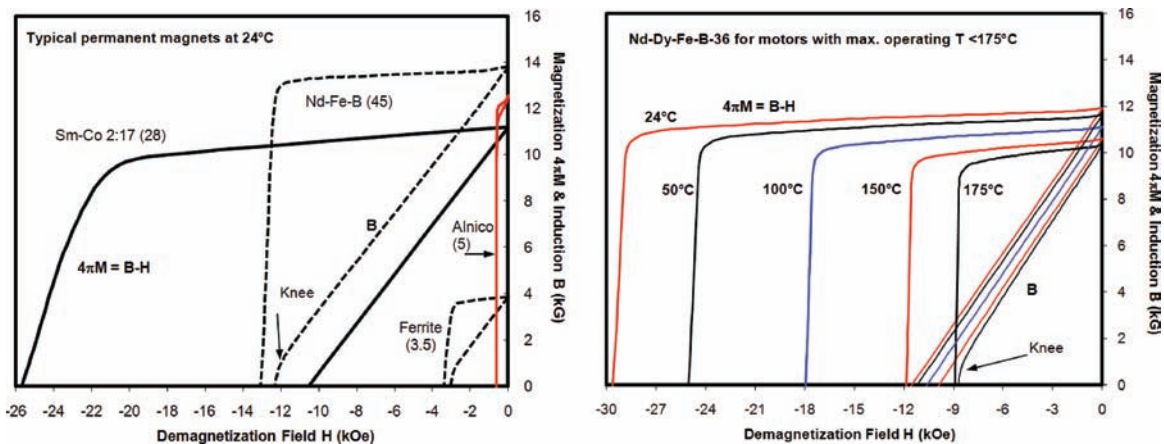


**Figure 4.** Demagnetization curves in the 2nd quadrant for four major permanent magnets (left) and at various temperatures for Nd-Dy-Fe-B used for motors (right). The  $(BH)_{\text{max}}$  at 25 °C is in the parenthesis. Reproduced with permission.<sup>[21]</sup>

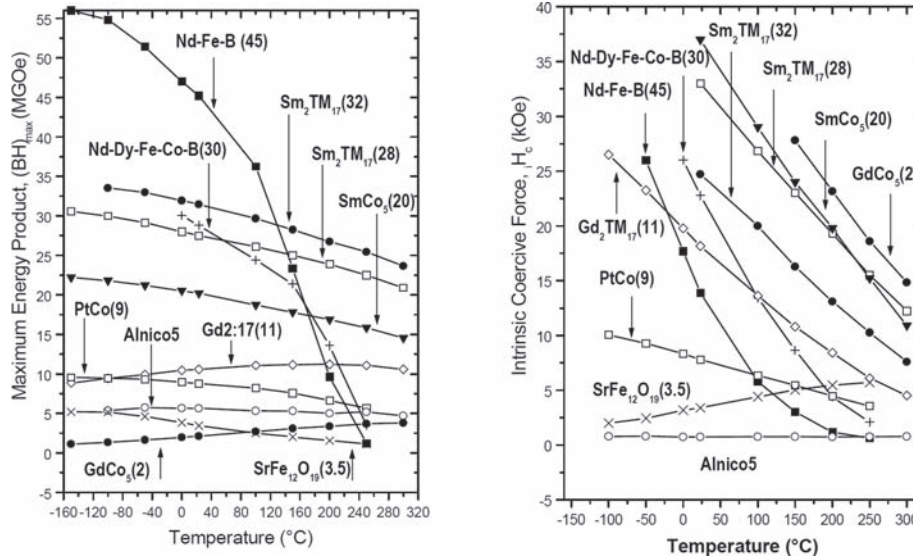


**Figure 5.** Magnetic properties of four magnets at up to 300 °C: energy product  $(BH)_{\max}$  versus  $T$  (left) and coercivity  $iH_c$  versus  $T$  (right).<sup>[20]</sup> The  $(BH)_{\max}$  at 25 °C is in the parenthesis. Reproduced with permission.<sup>[20]</sup> Copyright 2000, IEEE.

300 °C, making ferrite a relative good material for motor applications. With the exception of ferrite, all other magnets shown in Figure 5 have negative temperature coefficients of coercivity.

There are other considerations for permanent magnetic materials for energy related applications, including the load line for the magnets. The load line, also called the permeance coefficient, is only related to the geometry of the magnet. Figure 6 shows the demagnetization curves at 25 to 200 °C in 25 °C increments for an Nd-Dy-Fe-B magnet that can be used for hybrid vehicle motors. The figure also shows the load lines with

corresponding dimensions for cylindrical magnets. The load line intersects with the  $B$  curve ( $B$  vs  $H$ ), and the crossing point of the two lines is the operating point of the magnet,  $B_d/H_d$ .  $H_d$  is the demagnetization field and  $B_d$  is the induction  $B$  at  $H_d$ . The operating points for different temperatures are listed in Table 2, and the points in the shaded cells are not suitable for motor applications since they are near the knees of the  $B-H$  curves, where the magnet is vulnerable to demagnetization during the dynamic operation. One example can be used to explain a load line shown in Figure 6: the disc magnet with the length

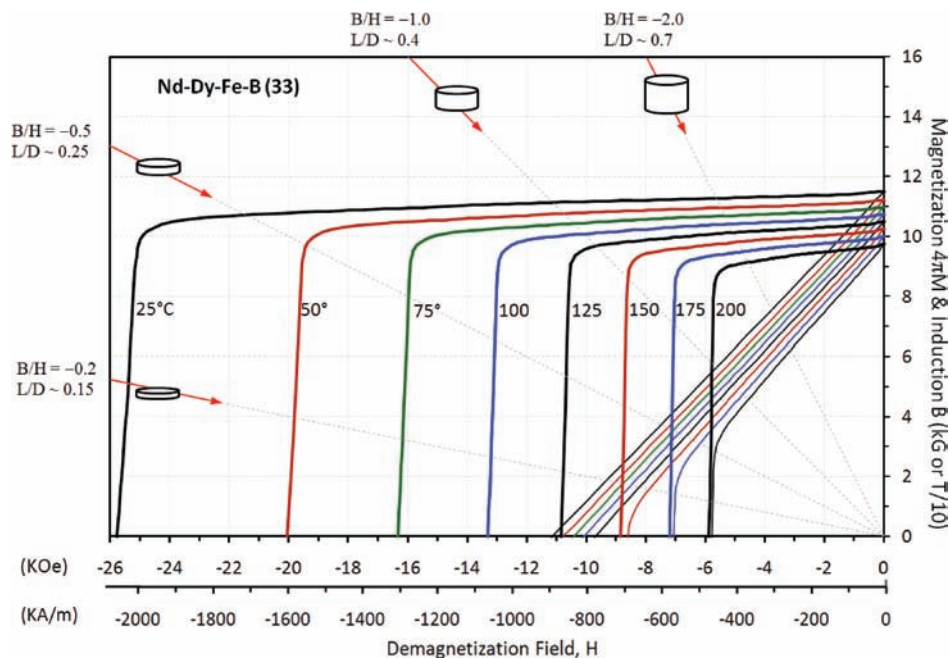


**Figure 6.** Demagnetization curves at 25 to 200 °C for an Nd-Dy-Fe-B magnet and the load lines with corresponding dimensions for cylindrical magnets. Reproduced with permission.<sup>[21]</sup>

**Table 2.** The operating point  $B_d/|H_d|$  for each operating temperature.

| Load line   |       | Operating point $B_d/ H_d $ (in kG/kOe) |          |          |         |         |         |         |         |
|-------------|-------|---|----------|----------|---------|---------|---------|---------|---------|
| $ B_d/H_d $ | $L/D$ | 25 °C                                   | 50 °C    | 75 °C    | 100 °C  | 125 °C  | 150 °C  | 175 °C  | 200 °C  |
| 0.2         | ≈0.15 | 1.80/9.4                                | 1.76/9.1 | 1.72/8.8 | 1.7/8.7 | 1.6/8.2 | 1.5/7.9 | 1.3/6.9 | 1.1/5.8 |
| 0.5         | ≈0.25 | 3.75/7.5                                | 3.7/7.2  | 3.6/7.1  | 3.4/6.8 | 3.2/6.6 | 3.1/6.4 | 3.0/6.2 | 2.8/5.6 |
| 1.0         | ≈0.4  | 5.7/5.7                                 | 5.6/5.6  | 5.4/5.4  | 5.2/5.2 | 5.1/5.1 | 5.0/4.9 | 4.8/4.8 | 4.7/4.7 |
| 2.0         | ≈0.7  | 7.5/3.8                                 | 7.4/3.7  | 7.2/3.6  | 7.1/3.5 | 6.9/3.4 | 6.7/3.3 | 6.4/3.2 | 6.2/3.1 |

\* The operating points in the shaded cells are not suitable for motor applications.

over diameter ratio ( $L/D$ ) of 0.15 has a load line with  $|B_d/H_d| = 0.2$ , and the operating point is 1.5 kG/7.9 kOe at 150 °C. This magnet is not stable when the operating temperature is higher than 150 °C because the operating points are near or below the knees of the  $B$  curves at 150 °C to 200 °C. For design engineers, this thin magnet should not be used at temperatures higher than 125 °C if safety is a factor under consideration.

## 2.2. World Market for Permanent Magnetic Materials

NdFeB magnets, in particular, have significantly impacted the development of computer peripherals such as voice coil motors and actuators, both in down-sizing and in enhancing their performance characteristics. For example, in 1984, computer disk drives of ≈10 MB size with random access time of over 60 ms were the norm. Today, external hard drives of much smaller physical dimensions but with a storage capacity of a few hundred GB, running at speeds up to 7200 rotations per minute (rpm) and with seek times of ≈8 to 12 ms have become common. More importantly, these high-performance drives are available at affordable costs. These extraordinary developments are partly attributable to the availability of magnets with energy products in excess of 50 MGOe. The production of NdFeB sintered magnets has steadily increased from about 6000 tons in 1996 to about 63 000 tons in 2008 (see Figure 7 and Table 3).<sup>[22]</sup> The volume of

these magnets manufactured in China, Japan, USA, and Europe together with their value (US dollars (US\$)) and price during the past decade are shown in Table 3. It is interesting to note that almost 80% of this strategic material is actually produced in China and manufacture in the US has ceased since 2004.

The world market for permanent magnets was estimated at ≈\$8 billion in 2007 and is predicted to be \$11 billion by 2010, with 34% hard ferrite, 65% rare earth magnets, and 1% Alnico. The growth rate of total permanent magnets is estimated to be ≈12% annually.<sup>[22]</sup> The fastest growing market is for Nd-Fe-B-based magnets with high energy product, which would capture 62% market share in 2010. The dominant growing area of permanent magnetic materials is the energy-related applications.

Design, development, and manufacture of consumer electronics goods, such as DVDs, iPods, cameras, sensors, and cell phones, are taking place at a rapid pace. All these devices include components that utilize permanent magnets, such as the vibratory motor in a cell phone. High-energy magnets enable the design of these miniaturized devices. Such a miniaturization strongly impacts the reduction in electrical power consumed in the operation these devices, either from the mains or through the rechargeable batteries. Thus, these devices now operate at high energy efficiencies. Large quantities of NdFeB magnets are used in the construction of battery-operated tools, magnetic resonance imaging (MRI) units, electric bicycles (EB), electric-assisted vehicles (EAV), speakers, magnetic separation units,

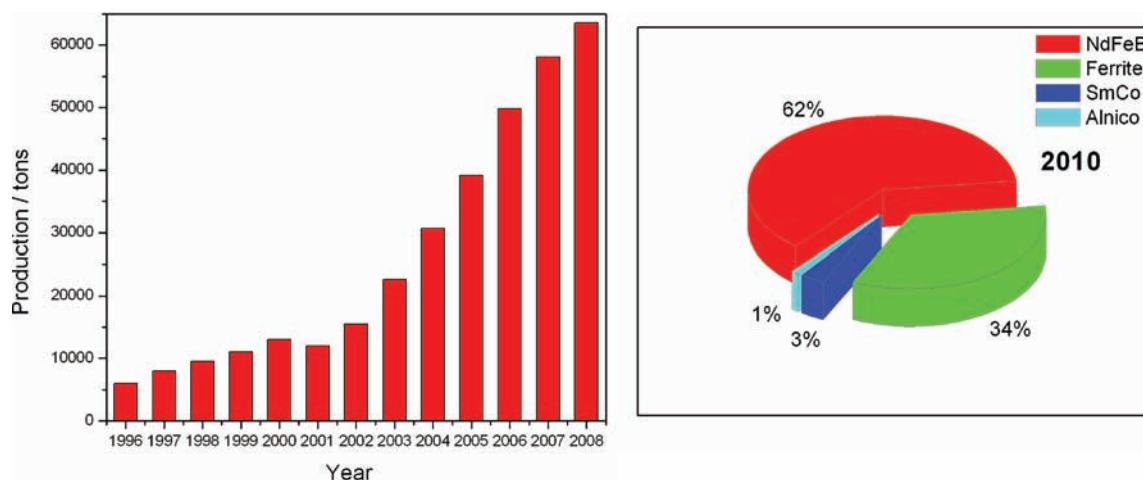


**Figure 7.** Output of NdFeB permanent magnets during the past ten years (left)<sup>[22]</sup> and predicted percentage sales (\$) for 2010 of the major permanent magnets in the world (right).<sup>[23]</sup>

**Table 3.** Output (in tons), sales value (in US\$  $\times 10^8$ ), and price (US\$ per kg) of NdFeB sintered magnets in China, Japan, USA, and Europe from 2003 to 2008.<sup>[22]</sup>

|                      | 2003    | 2004    | 2005    | 2006    | 2007    | 2008    |
|----------------------|---------|---------|---------|---------|---------|---------|
| <b>China Output</b>  | 15 550  | 22 910  | 30 160  | 38 220  | 45 100  | 49 880  |
| Value                | 5.598   | 7.7894  | 9.9528  | 13.377  | 18.04   | 20.9496 |
| Price                | 36      | 34      | 33      | 35      | 40      | 42      |
| <b>Japan Output</b>  | 6200    | 7000    | 8500    | 10 500  | 11 800  | 12 600  |
| Value                | 5.084   | 5.74    | 7.14    | 9.345   | 11.21   | 12.348  |
| Price                | 82      | 82      | 84      | 89      | 95      | 98      |
| <b>USA Output</b>    | 100     | –       | –       | –       | –       | –       |
| Value                | 0.08    |         |         |         |         |         |
| Price                | 80      |         |         |         |         |         |
| <b>Europe Output</b> | 810     | 800     | 950     | 1080    | 1210    | 1100    |
| Value                | 0.6561  | 0.648   | 0.779   | 0.9398  | 1.1253  | 1.067   |
| Price                | 81      | 81      | 82      | 87      | 93      | 97      |
| <b>Global Output</b> | 22 660  | 30 710  | 39 160  | 49 800  | 58 110  | 63 580  |
| Value                | 11.4181 | 14.1774 | 17.8718 | 23.1396 | 30.3753 | 34.3646 |
| Price                | 50.4    | 46.2    | 45.1    | 46.47   | 52.3    | 54.1    |
| China/Global         | 68.6%   | 74.6%   | 76.1%   | 76.7%   | 77.6%   | 78.5%   |
| Japan/Global         | 27.4%   | 22.8%   | 21.5%   | 21.1%   | 20.3%   | 19.8%   |
| USA/Global           | 0.4%    | –       | –       | –       | –       | –       |
| Europe/Global        | 3.6%    | 2.6%    | 2.4%    | 2.2%    | 2.1%    | 1.7%    |

etc. This market segment is shown in **Table 4** for China. The market can be divided into three groups; the first one is termed the high-tech; the second group as the traditional and the third one as the low grade. It is interesting to note that the first group has experienced a four-fold expansion while the second group (traditional) has nearly doubled during the past five years.

Today ferrite magnets have the largest share in terms of tonnage in energy-related applications, which is attributed to

their low price. Based on the sales data in Figure 7, we estimate annual usage is  $\approx 433$  kilotons for ferrite magnets and  $\approx 68$  kilotons for Nd-Fe-B magnets. As described earlier, the invention of ferrite in 1946 revolutionized the design of motors and generators. Despite the low-energy product (less than 10% of that of Nd-Fe-B magnets) today ferrite is still the choice of many engineers because of its low price. For the motors used for hybrid vehicles, Dy partially substitutes Nd in order

**Table 4.** Distribution of NdFeB magnet applications in China (in tons).<sup>[22]</sup>

| Application            | 2003          | 2004          | 2005          | 2006          | 2007          |
|------------------------|---------------|---------------|---------------|---------------|---------------|
| MRI                    | 360           | 560           | 760           | 1110          | 1800          |
| VCM                    | 200           | 350           | 530           | 995           | 1300          |
| CD pick-up             | 840           | 1150          | 1540          | 2305          | 2515          |
| DVD/CD ROM             | 1250          | 1800          | 2440          | 3290          | 4060          |
| Mobile phone           | 360           | 680           | 950           | 1910          | 3160          |
| Coreless tool          | 960           | 1250          | 1490          | 1990          | 3160          |
| EB+EAV                 | 1330          | 2280          | 3420          | 4560          | 5860          |
| Subtotal (high-tech)   | 5300          | 8070          | 11 130        | 16 160        | 21 855        |
| Speaker                | 3850          | 5730          | 7540          | 9560          | 11 280        |
| Separator              | 2270          | 3420          | 4090          | 3950          | 3610          |
| Magnetizer             | 1030          | 1070          | 1210          | 1150          | 990           |
| Subtotal (traditional) | 7150          | 10 220        | 12 840        | 14 660        | 15 880        |
| Low-grade use          | 2550          | 3840          | 4980          | 6080          | 6320          |
| Other                  | 550           | 780           | 1210          | 1320          | 1045          |
| <b>Total</b>           | <b>15 550</b> | <b>22 910</b> | <b>30 160</b> | <b>38 220</b> | <b>45 100</b> |

to increase the coercivity ( $H_c$ ) to a level sufficient for high-temperature applications. The disadvantages of this are the reduction in the energy density,  $(BH)_{\max}$ , caused by the antiparallel coupling between Dy and Fe in the  $(\text{Nd,Dy})_2\text{Fe}_{14}\text{B}$  unit cell<sup>[24]</sup> and the rarity of Dy.<sup>[19]</sup> It is estimated that currently 97% of Dy rare-earth metal supply worldwide (1200 tons in 2008) is of Chinese origin.<sup>[25]</sup> Metal prices in 2009 show that Dy costs  $\approx 8$  times as much as Nd metal.<sup>[26]</sup> In order to keep the cost as low as possible and energy product as high as feasible, different applications use different grades of Nd-F-B-based magnets, as indicated in the insert of Figure 3. Common perception usually is that Sm-Co is much more expensive than the Nd-Fe-B magnets, since the Sm metal is more expensive than Nd and the production process for Sm-Co is more complex than that for Nd-Fe-B. The raw material cost of Nd-Dy-Fe-B is  $\approx \$20$  per kg, higher than that for Sm-Co 2:17 metals,  $\approx \$18$  per kg, as listed in Table 5. The longer manufacturing process for Sm-Co makes its price  $\approx 15\%$  higher than Nd-Dy-Fe-B's; however, if a higher acceleration and a higher fuel efficiency (requires higher operating temperature) for certain electric cars are the goals, Sm-Co could actually be an alternative (compare Figure 5 (left)). Heavy rare-earth elements like dysprosium and to some extent terbium are key components in producing RPMs that show the required temperature stability for motor applications. Looking at the supply situation, a strategy and novel microstructures for RPMs are required to reduce the use of Dy. Another important issue for the future is the recycling of RPMs, again to ensure a stable supply of rare-earth metal sources. For this purpose, hydrogen-assisted processing of RPMs could be very advantageous.<sup>[27–29]</sup> The hydrogen decrepitation process (HD)<sup>[30]</sup> could be used in the recycling of  $\text{SmCo}_5$ ,  $\text{Sm}_2(\text{Co,FeCu,Zr})_{17}$ , and NdFeB-type magnets. The growth of electric vehicles and with increasing environmental legislation, which is likely to demand better energy efficiency, and more resourceful use of materials including recycling, especially for automotive applications where “end of life” rules are already being implemented. Such measures can be justified in terms of environmental impact (metal contamination of landfill sites), energy saving ( $\text{CO}_2$  reductions), and resource depletion.

### 2.3. Torque and Efficiency

Gieras and Wing<sup>[31]</sup> point out that “the use of permanent magnets in the construction of electrical machines result in the following benefits: (a) no electrical energy is absorbed by the field excitation system and thus there are no excitation losses which means substantial increase in efficiency; (b) higher torque

and/or output power per volume (of the machine) than when using electromagnetic excitation, and (c) better dynamic performance than motors with electromagnetic excitation (higher magnetic flux density in the air gap)”.

In addition to the developments in the permanent magnets, there has been a substantial progress in semiconductor electronics resulting in the availability of switching devices, such as MOSFETs (metal oxide semiconductor field-effect transistors) and IGBTs (insulated-gate bipolar transistors), which are used to commutate the motors. Further, developments in power electronics enable the design and manufacture of intelligent controllers to operate electromechanical devices. Computer software tools employing finite-element analysis techniques have assisted in rapidly prototyping electromechanical devices. Thus, the synergistic advances in these fields have enabled the rapid growth of the permanent magnet motor industry.

The electromagnetic interaction between the magnetic flux produced by a permanent magnet with a flux density,  $B$ , and the electrical current flowing through a surrounding coil of length,  $L$ , and area of cross section,  $A$ , carrying current with a current density,  $j$ , results in the generation of torque  $\tau = BjrAL$ , where  $r$  is the length of the torque arm. Generally, the magnetic flux is focused to interact effectively with the current through the use of a soft magnet, such as soft steel, placed within the available space envelope.<sup>[32]</sup> During operation of a motor, eddy currents, hysteretic effects, and mechanical friction all contribute to electric losses in the form of heat. The ratio between the mechanical power,  $P_{\text{mech}}$ , derived from running the motor at an angular velocity,  $\omega$ , and the electrical power,  $P_{\text{elec}}$ , provided into the motor is the efficiency,  $\eta$ , of the motor. Thus,  $\eta = (P_{\text{mech}})/(P_{\text{elec}}) = (\tau\omega)/(VI)$ . In this expression,  $V$  is the voltage supplied to the motor that produces a current  $I$ . Torque versus speed or torque versus current and the efficiency of the motor describe the basic performance characteristics of a motor. The design engineers have to a) maximize the flux density,  $B$ , by a suitable selection of the permanent magnet as well as the soft magnet material; b) maximize the interaction between the flux lines of the magnet and the current flowing through the surrounding wire by optimizing the geometry of the device; and c) minimize the losses due to eddy currents, hysteresis, and frictional effects and, if necessary, find an effective means to withdraw the heat produced in the motor by e.g., mounting it on a heat sink.

Gieras and Wing<sup>[31]</sup> compared the performance of a small three-phase, four-pole, 1.5 kW, 50 Hz cage-induction motor with that of a rare-earth permanent magnet (PM) brushless motor. The full-load efficiency of the former is about 75% while that of the latter is nearly 88%. Thus, the induction motor

**Table 5.** Cost of raw materials of the two types of magnets (price based on July 2009 data).<sup>[26]</sup>

|            | Nd-Dy-Fe-B               |      |       |      | Sm-Co (2:17)             |      |      |     |     |
|------------|--------------------------|------|-------|------|--------------------------|------|------|-----|-----|
|            | Nd                       | Dy   | Fe    | B    | Sm                       | Co   | Fe   | Cu  | Zr  |
| at%        | 10.00                    | 4.00 | 80.00 | 6.00 | 13.3                     | 59.6 | 19.3 | 5.7 | 2.1 |
| wt%        | 21.77                    | 9.81 | 67.44 | 0.98 | 28                       | 49.1 | 15.1 | 5.1 | 2.7 |
| Price (\$) | 4.4                      | 14.2 |       |      | 5.9                      | 9.0  |      | 0.5 | 0.5 |
| Total cost | $\approx \$20/\text{kg}$ |      |       |      | $\approx \$18/\text{kg}$ |      |      |     |     |

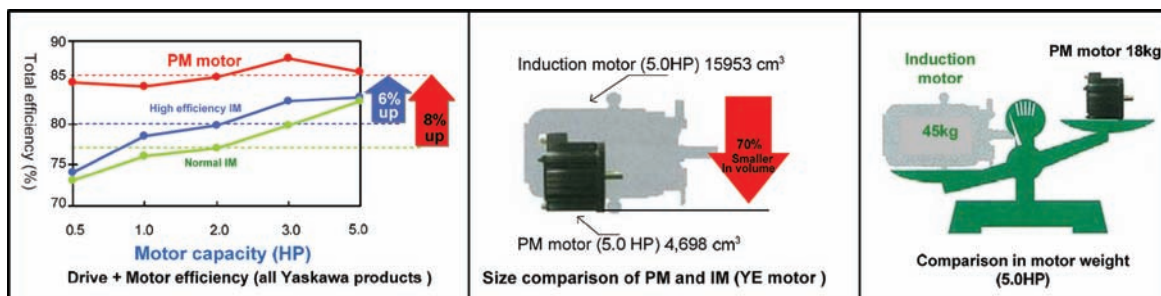


Figure 8. Some advantages of a PM motor over an induction motor (IM). Reproduced with permission.<sup>[33]</sup>

draws nearly 2000 W of electricity and the PM motor draws only 1704 W. The power savings is 296 W (or  $\approx 15\%$ ) per motor. Figure 8 shows some of the advantages of PM motor versus induction motors.

Honkura<sup>[34]</sup> demonstrates that the enhancement in the energy efficiency of a motor using rare-earth bonded magnet is nearly 13% compared to a ferrite magnet motor, both operating at the maximum 400 W. The power density of the rare-earth permanent magnet motor was improved nearly twofold compared to the ferrite motor.

Electric vehicles, hybrid as well as plug-in, employ brushless motors. Proper design of such motors and the control electronics is now a very important area of worldwide research and development. Key objectives are to a) design light-weight, high torque-to-weight ratio motors, b) achieve high efficiency throughout the operational range, c) provide reliable control, d) have rugged construction, e) provide low maintenance requirements, and f) supply the customers at low cost. It is also important to note that electric motors have high torque at low speeds. In contrast, in internal combustion engines the torque increases with speed until reaching an optimum power level and then falls sharply. Thus, the permanent magnet motors offer a number of benefits in furthering this mobility application.

The possibilities of producing exchange-coupled permanent magnets that offer the ability to exhibit energy products in excess of  $\approx 60$  MGOe are being investigated by a number of researchers around the world. However, in the case of conventional brushless, slotted motors (which are typically employed in

many applications), the torque levels off at about 40 MGOe due to the flux saturating the soft magnet that is used in the core. Simizu et al.<sup>[35]</sup> modeled the possibilities of designing brushless motors that are slotless and demonstrated the overwhelming advantages of such designs in the further enhancement of torque using permanent magnets with potentially much improved high-energy products. A nearly 25% increase in the torque of slotless, brushless permanent magnet motors over the slotted designs at about 60 MGOe, with a further potential for such increases at higher-energy products of permanent magnets, have been predicted. Such designs will also result in an increase in energy efficiency. Further advantages of adopting high energy density magnets include higher torque-to-weight ratio and reduction in noise and clogging.

#### 2.4. Renewable Energy Generators: Wind Power and Magnetic Materials

Wind power is the fastest growing sector within the renewable power generation. According to the World Wind Energy Association (WWEA), worldwide wind power capacity was 159 213 MW in 2009. As shown in Figure 9, wind power capacity has doubled every three years in the last decade and is predicted to be around 1 900 000 MW in 2020.<sup>[36]</sup> A typical commercial wind turbine consists of three blades connected to an asynchronous generator via a gearbox, thus transforming the mechanical power into electrical power. Asynchronous generators are constructed with

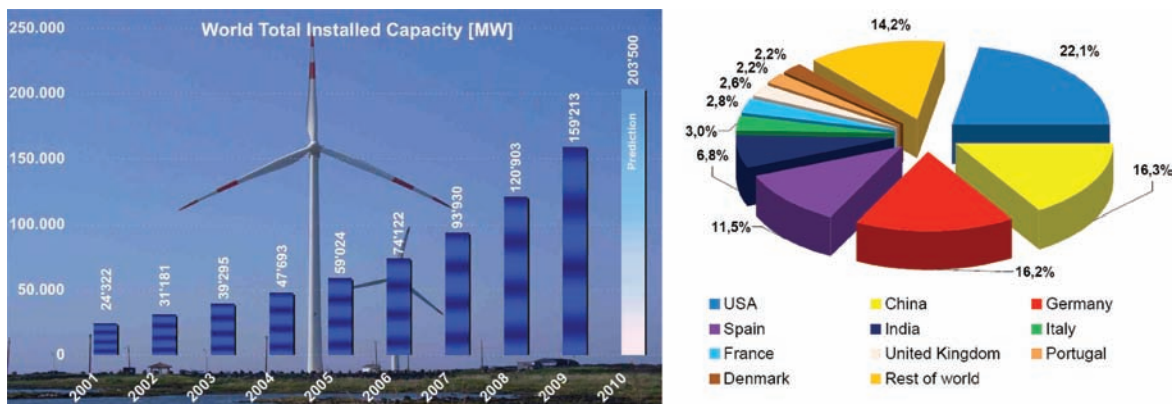


Figure 9. World total installed wind energy during the last decade (left) and country share of total capacity 2009. Reproduced with permission.<sup>[36]</sup> Copyright 2010, World Wind Energy Association.

soft magnetic lamination and iron and copper armature windings with the excitation field provided by copper coils.

Various wind turbine concepts have been developed and built to maximize the energy harnessed, to minimize the cost, and to improve the power quality. Turbine concepts can be classified with respect to the rotational speed, the power regulation, and the generator system. When considering the construction of the generator system, the turbines can be divided into direct-drive and geared concepts. Generator systems can be separated into the electrically excited (EE) machine and the permanent magnet (PM) machine. The direct-drive generator system, especially direct-drive PM generator system, is superior in terms of the energy yield, reliability, and maintenance.<sup>[37]</sup> Because of reliability issues and high servicing schedules of gearboxes, turbine producers are developing direct-drive (DD) generators, which allow power transformation without a gear. This has resulted in a shift to synchronous generators because of the higher torque density with the excitation field provided by the permanent magnet. New designs use Nd-Fe-B permanent magnets in the synchronous generators (PMSG). As shown in **Figure 10**, four permanent magnet Nd-Fe-B generators are major components in advanced wind turbines. A comparison of the new design with PM generators and a conventional generator yields drastic differences in volume and weight<sup>[38]</sup> as well as higher operating efficiency, higher torque density, 50% lower internal heat generation, and easier assembly and maintenance.<sup>[39,40]</sup> Compared to a geared system, the torque can be 100 times larger for a DD generator.

Permanent magnet generators should have more advantages compared to conventional generators if the design of the generators can be revolutionized by fully utilizing the high-energy products of RPMs. The designs for the PM generators today are more or less similar to the configurations developed for using hard ferrite magnets invented in 1946, which revolutionized the design of inductors, transformers, motors, and generators. RPMs, such as Sm-Co and Nd-Fe-B, have 8 to 15 times the energy product compared to the ferrites. The high-energy product should significantly benefit the innovative design with tremendous performance enhancement. However, reports of multi-megawatt wind turbine showed similar generator configurations, even when these very different magnets ferrites and Nd-Fe-B would be used.<sup>[39]</sup> For example, a 144-pole radial-flux PM generator would use 2948 kg of ferrite and a 144-pole radial-flux PM generator would use

2918 kg of Nd-Fe-B. Apparently these proposed generators do not fully utilize the high energy density of RPMs and therefore a new design of PM generators is needed.

A 3 MW DD generator uses about 1.5 tons of RPMs; with this the magnetic material represents a significant fraction of the generator costs. Due to the consumer demand for low cost and long lifespan wind turbines, the permanent magnet components represent an important trade-off between minimizing volume and protection against irreversible demagnetization due to electrical faults or excessive heating. As demand increases for wind turbines and permanent magnet technologies emerge across industry sectors, a high demand for rare-earth magnets could result in an increased material price and consequent challenges for the economical feasibility.

## 2.5. Energy Efficient Electric Machines: Electric and Hybrid Vehicles

The year 2009 was the 100th anniversary of the granting of the first US hybrid car patent or “Mixed Drive for Automobiles” (**Figure 11**) as it was described by the German inventor Henri Pieper.<sup>[42]</sup> He says in his patent: “The invention... comprises an internal combustion or similar engine, a dynamo motor direct connected therewith, and a storage battery or accumulator in circuit with the dynamo motor, these elements being cooperatively related so that the dynamo motor may be run as a motor by the electrical energy stored in the accumulator to start the engine or to furnish a portion of the power delivered by the set, or may be run as a generator by the engine, when the power of the latter is in excess of that demanded of the set, and caused to store energy in the accumulator.” Pieper’s patent also included a rudimentary battery and engine management system. Unfortunately for Pieper, the year before his patent was granted the assembly lines for the first inexpensive mass-produced car based on the internal combustion engine, the Ford Model T, were under construction. By the 1930s, production of hybrids based on the Pieper system had ceased completely and the prevalence of the gasoline engine powered automobiles was cemented. Drivers controlled a magnetic-disc clutch that connected the engine to a DC-motor generator, or dynamo, which was in turn connected to a gear-set that turned the rear wheels via chain drive. Now, a century later, hybrid electric vehicles have re-emerged as a realistic alternative to the gas-only internal combustion vehicle. The basic concept of a parallel hybrid is in principle retained in today’s hybrids like the Toyota Prius (see **Figure 12**).

Currently more than 1.5 million HEVs are on the road. Apart from the worldwide environmental issues, this re-emergence has been driven by the multiple advances in magnetic materials, electrical machine design, power electronics, and battery/fuel cell technology. Electric or hybrid vehicles are being developed at an unprecedented pace<sup>[44]</sup> and their sales is expected to increase dramatically in the next five years. One of the three key components (besides the power control unit and battery) of the hybrid vehicles is the PM-electric motor. As described earlier, as is the case with PM generators, PM motors have many advantages compared to induction motors including compact size, high efficiency, light weight, and high torque. According

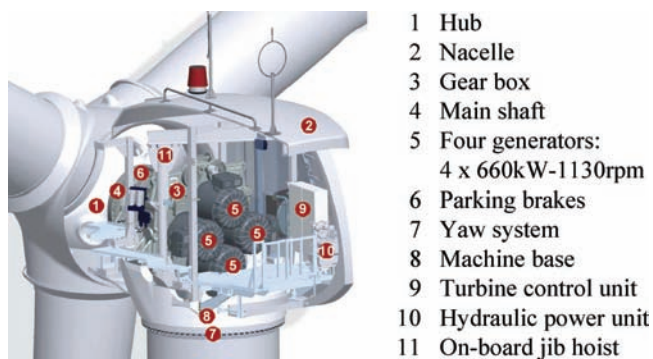


**Figure 10.** Clipper’s 2.5 MW wind turbine with four permanent magnet generators. Reproduced with permission.<sup>[41]</sup>

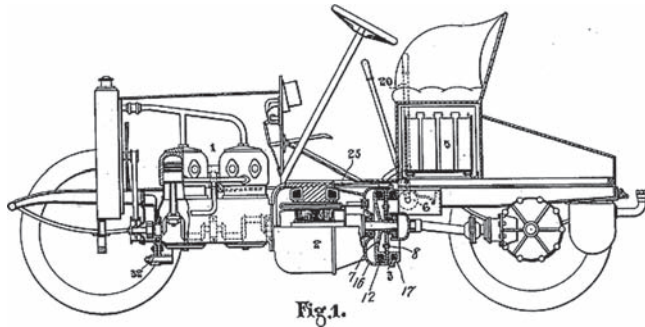


**Figure 11.** Picture from Henri Pieper's hybrid vehicle patent application from 1905.<sup>[42]</sup>

to Toyota, each hybrid Prius motor/generator uses  $\approx 1.3$  kg of Nd-Dy-Fe-B magnets.<sup>[43]</sup> The Toyota Hybrid System (THS) is a power train combining the series hybrid system with the parallel hybrid system in order to maximize the benefits of both. Developing energy-efficient machines and hybrid vehicles demands permanent magnets with high performance as shown in Figure 12.

One way to reach the goal of having the best fuel economy and acceleration in the marketplace is to develop new permanent magnets with higher energy product and good thermal stability at temperatures of 150–250 °C. Current hybrid vehicles use Nd-Dy-Fe-B magnets with  $(BH)_{\max} = 286.5 \text{ kJ m}^{-3}$  (36 MGOe) and intrinsic coercivity  $iH_c = 2400 \text{ kA m}^{-1}$  (30 kOe), stable at temperatures of about 180 °C. The value of  $iH_c$  is very important for such dynamic applications with elevated operating temperature because it is a key to resisting thermal demagnetization. The performance of a PM motor is directly related to the magnetic flux provided by the permanent magnets. The Prius PM motor consists of an eight-pole rotor with high coercivity Nd-Fe-Dy-B magnets inside. As shown in Figure 13, by arranging the permanent magnets in a V-shape rather than a flat-shape, the output power is increased from 33 to 50 kW ( $\approx 1.5$  times) and the drive torque is increased from 350 to 400 N-m ( $\approx 15\%$

higher). The increased performance results from higher magnetic flux density in the working gap, estimated at  $\approx 15\%$  using Ansoft's Maxwell 3D computer modeling.<sup>[45]</sup>

It is not a straight-forward calculation to determine the percent gain in motor efficiency resulting from the gain in energy density of the magnet  $(BH)_{\max}$ . Different design is required as the energy density of the magnet is increased because a higher magnetic flux from the magnets can cause localized magnetic saturation in certain areas if the design is not changed, and this will not increase the torque and output power of the motor. Many researchers reported their attempts to establish a method to estimate the torque of a motor.<sup>[46]</sup> These reports targeted different PM-rotor design rather than different energy densities of the magnets. To estimate the motor's improvement resulting from the increase in energy density of the magnets, Ansoft's RMxprt computer software was used for analyzing a four-pole surface-mounted PM motor,<sup>[45]</sup> as shown in Figure 14, using the magnets with energy products of 23, 36, and a fictitious 72 MGOe. The results are shown in Figure 15. When the same motor configuration is used, the starting torque ( $\text{rpm} = 0$ ) and output power are increased by 25–30% when  $(BH)_{\max}$  of the magnet is increased from 36 to 72 MGOe. However, we have to realize that a new design must be used when better magnets are used, as described earlier. According to our estimation, the torque and output power with 72 MGOe magnets could be increased by 70% compared to 36 MGOe magnets if an appropriate design were be used. The torque and the output power of the new design using 72 MGOe magnets are shown in the top plots in Figure 15.

## 2.6. Understanding and Controlling Microstructure on the Nanoscale

Various approaches are being examined in order to develop Dy-free Nd-Fe-B sintered magnets with high  $H_c$  for high-temperature applications.<sup>[47]</sup> In order to achieve this, it is

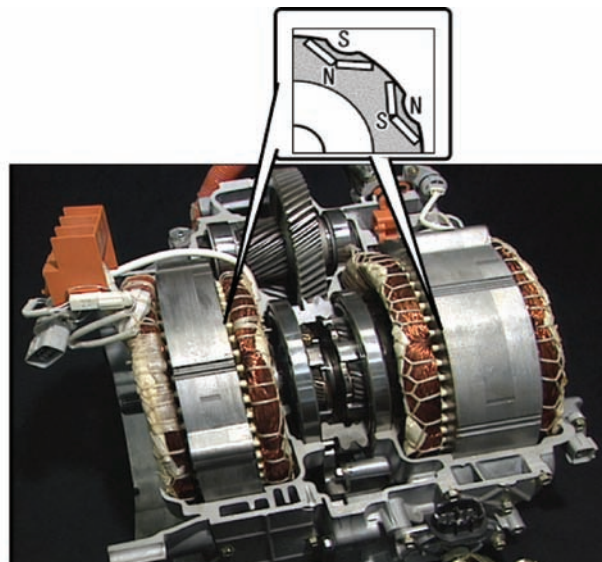
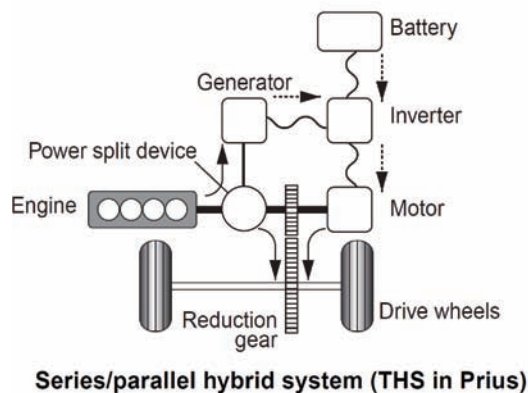


**Figure 12.** Prius' generator and motor. Reproduced with permission from Toyota Motor Corporation.<sup>[43]</sup>

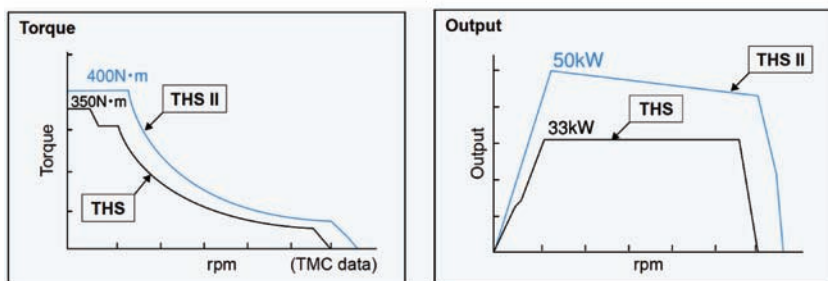


**Figure 13.** The effect of magnet arrangement on the performance of Prius PM motor/generator<sup>[43]</sup>; magnet arrangements in 8-pole rotors of THS motor (top left) and THS II motor (top right) and related torque (bottom left) and output (bottom right) for the two arrangements. Reproduced with permission from Toyota Motor Corporation.<sup>[43]</sup>

vital to understand the coercivity mechanism in Nd-Fe-B sintered magnets in greater detail. The Nd-rich phases and their distributions in the microstructure are critical for the  $H_c$  of the magnet, but currently  $H_c$  reaches only 20–30%<sup>[8]</sup> of the theoretical maximum (Brown's paradox<sup>[48]</sup>), which is the anisotropy field,  $H_A$ . This is because the nucleation of inverse magnetic domains occurs at a much lower magnetic field than the anisotropy field starting from the grain boundaries, where the anisotropy of the  $Nd_2Fe_{14}B$  phase is expected to be locally decreased due to the presence of defects, roughness, or incomplete wetting by the paramagnetic Nd-rich grain boundary phase. Since the coercivity of Nd-Fe-B magnets is strongly influenced by the microstructure, especially the magnetic isolation of the ferromagnetic grains and the grain boundary structure and microchemistry, important microstructure changes are expected to occur during the postsinter annealing, particularly at the grain boundaries.<sup>[49]</sup> However, there is no definite work that has characterized the structure and chemistry of the grain boundaries of Nd-Fe-B sintered magnets. Magnetically isolated single-domain particles are expected to give rise to much higher

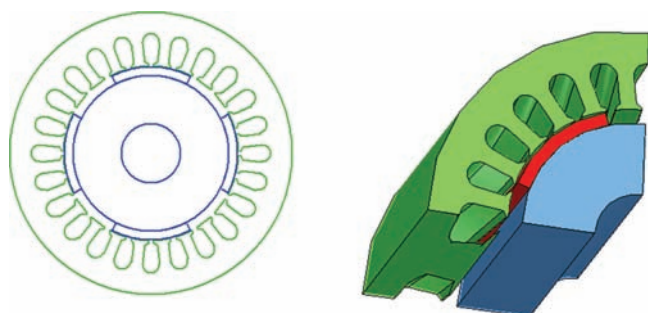


**Figure 14.** The 2D and 3D model of a four-pole surface PM motor used for computer modeling (the copper windings are hidden).<sup>[21]</sup>

coercivity, but such a microstructure has never been achieved in the Nd-Fe-B system. The approach of multiscale characterization of sintered Nd-Fe-B commercial magnets is illustrated in **Figure 16**.

On another front, research in producing exchange-coupled nanocomposite permanent magnets has achieved remarkable progress.<sup>[50]</sup> By adding nanoscale soft magnetic phases into a hard magnetic phase matrix, the energy density of the composite can be greatly enhanced due to the interphase exchange coupling,<sup>[51]</sup> while the cost of the magnets can be simultaneously reduced by the lower rare-earth contents of the composites compared to their single-phase counterparts. A bottom-up approach has been applied to produce nanocomposite magnets based on rare-earth transition metal compounds starting with preparation of the hard and soft magnetic nanoparticles. **Figure 17a,c** show the nanoscale particles produced by surfactant-assisted ball milling.<sup>[52,53]</sup> The particles are magnetically anisotropic and can be aligned in a magnetic field to form anisotropic bulk magnets. **Figure 17d–f** show the Fe-Co-based soft-phase distribution in a bulk  $SmCo_5/Fe(Co)$  nanocomposite processed by severe plastic deformation and warm compaction.<sup>[54]</sup> In the isotropic bulk magnets processed using these techniques, substantial energy density enhancement has been achieved while  $\approx 30\%$  fewer rare-earth elements were used.<sup>[54]</sup> It is predicted that success in producing anisotropic nanocomposite magnets will lead to a revolutionary change in permanent magnetic materials development and applications.

### 3. Soft Magnetic Materials

Soft magnetic alloys have played a key role in both power generation and conversion for the electrical grid, as one can see from the heavy application of soft magnets in transformers. The need for efficient generation, transmission, and distribution of electric power is ever growing; however, at the same time the annual electric losses are outpacing annual increases in electricity consumption. While the increased production of energy from renewable sources is extremely important, the reduction of electrical losses also needs to be addressed. At present, the electrical grid consists of localized stations for the generation of electricity. In the USA, electricity is converted to high-voltage AC current at voltages between 138 and 765 kV and transmitted to substations near its end-use location. The voltage is then stepped down to lower values (between 13 kV and 120 V) for distribution to industrial and residential consumers. These generation, transmission, and distribution systems are aging, inefficient, and inadequate to meeting the future energy needs of the USA without significant changes in operation and infrastructure. For these reasons, advanced electric storage systems, smart controls, and power electronics for AC–DC conversion are technologies that are being supported to revolutionize the way

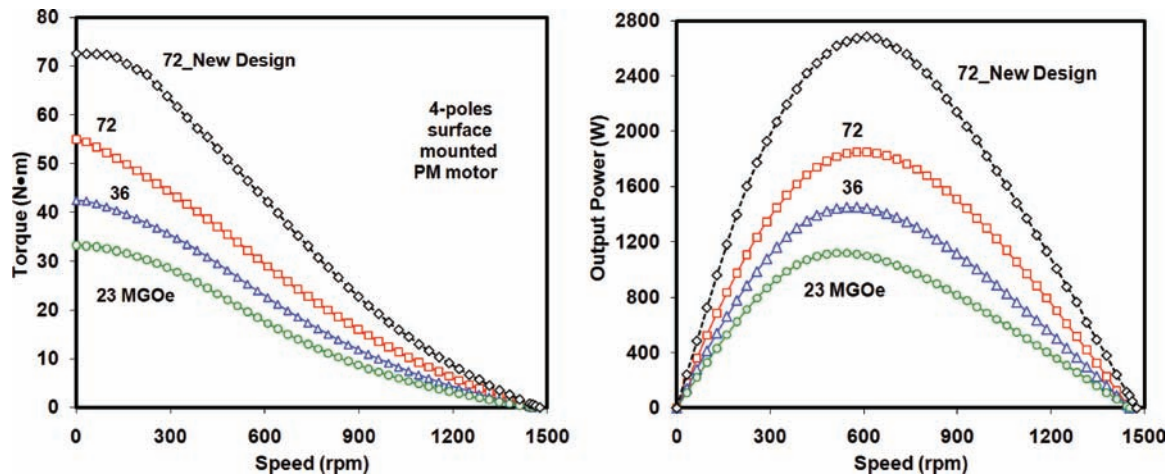


**Figure 15.** The effect of the energy products of the magnets on a PM motor performance (all magnets have linear  $B-H$  demagnetization curves in the second quadrant suitable for dynamic application). Torque vs speed (left) and output power vs speed (right).<sup>[45]</sup>

we deliver power.<sup>[55]</sup> These so-called “smart-grid” technologies, using an array of advanced materials and devices, will provide more efficient, affordable, and sustainable energy use for the long term.<sup>[56]</sup> On the electricity generation side, soft magnetic materials are especially important to maintaining an efficient smart grid. For example, soft magnets have important roles in wind energy technologies for generation using advanced induction motors and for conversion using power converters and/or power transformers. The architecture of modern wind turbines include the generator in the nacelle (the enclosure attached to the rotor blades at the top of the turbine tower).<sup>[57,58]</sup> Due to the

desire to increase the capability of these devices, induction generators housed in the nacelle must be given higher energy densities, which can be accomplished with improved soft magnetic materials and/or permanent magnetic materials if PM-motor designs are employed.

About 9% of the electricity generated is lost as heat during transmission and distribution.<sup>[59]</sup> While high voltage is necessary for low losses in electrical transmission, DC transmission has lower losses than AC transmission. This is one reason that the smart grid has been discussed in terms of high-voltage direct-current (HVDC) transmission. The expense of the HVDC

converter stations limits the implementation of this more energy-efficient technology to transmission. For this reason, the implementation of smart grid technology will continue to require improved energy efficiency for rectifiers, inverters, and transformers using advanced soft magnetic materials. In present devices, losses can be as low as 0.25% for some large utility transformers, however, they may also be as high as 15% for small consumer electronics “power bricks”. In these applications, losses come from a variety of sources including winding resistance, eddy currents, stray fields, hysteresis, mechanical losses, magnetostriction, and cooling systems. Of these, eddy currents, hysteresis, and magnetostriction are important soft magnetic parameters. Due to their central role in these devices, soft magnetic cores with lower core losses (including contributions from hysteretic, magnetostrictive, and eddy current sources), higher magnetization, and improved cost effectiveness will be key components for improved energy efficiency.

Soft magnetic materials come in many forms ranging from soft iron, used in powder core inductors, to silicon steel laminates and nanocrystalline or amorphous tape wound cores for transformers, and to soft ferrites for electromagnetic interference (EMI) filters. The materials selection is important for

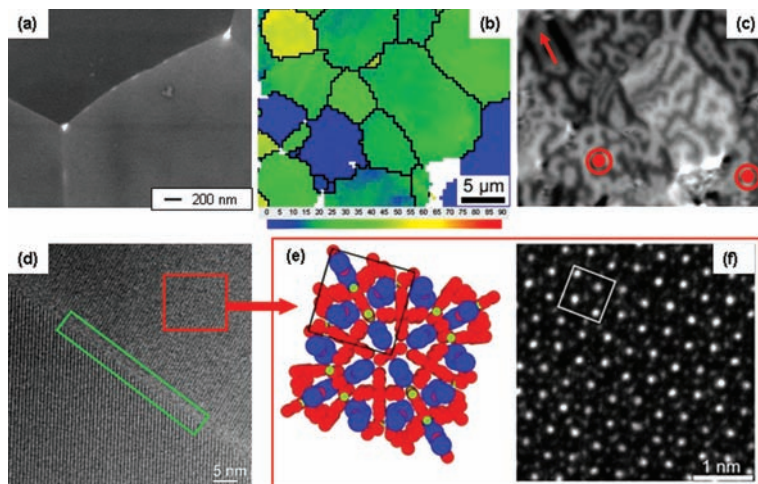


**Figure 16.** Multiscale characterization of sintered Nd-Fe-B commercial magnets: a) Backscattered electron contrast scanning electron microscopy (SEM) image showing the hard magnetic  $\text{Nd}_2\text{Fe}_{14}\text{B}$  matrix grain well-separated by a thin Nd-rich intergranular phase (white contrast). b) Electron backscattering diffraction (EBSD) image quantitatively showing the local variation in orientation of the different grains. c) optical Kerr microscopy showing the corresponding magnetic domain structure of the same area. d) Transmission electron microscopy (TEM) image showing the amorphous Nd-rich intergranular phase of about 1 nm thickness (from top left to bottom right). Panels (e,f) show schematically and in atomic resolution the  $\text{Nd}_2\text{Fe}_{14}\text{B}$  matrix phase. Courtesy: T. G. Woodcock, IFW Dresden.

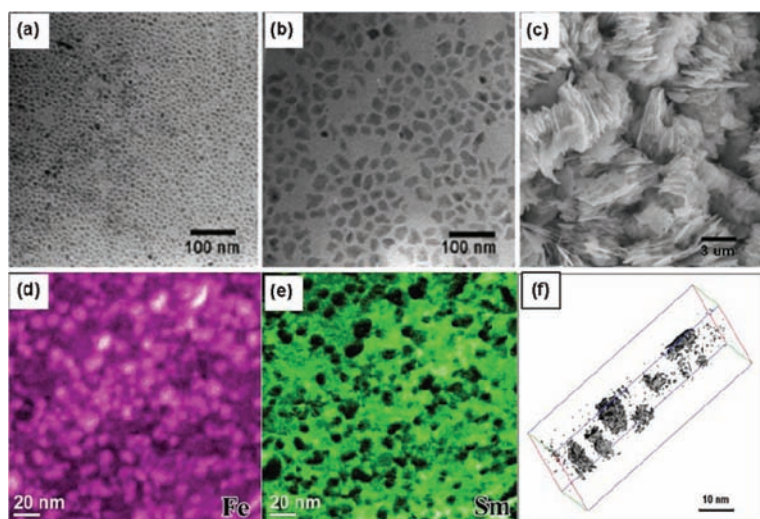


**Figure 17.** Nanoscale hard magnetic particles and composites. a) TEM image of  $\approx 6$  nm particles of  $\text{Sm}_2\text{Co}_{17}$  produced by surfactant-assisted ball milling; b) TEM image of  $\approx 20$  nm particles prepared in the same method with size selection; and c) SEM image of the  $\text{SmCo}_5$  plate-like particles obtained by surfactant-assisted ball milling. d) Energy-filtered TEM image showing Fe distribution and e) Sm distribution in a  $\text{SmCo}_5/\text{Fe}$  nanocomposite bulk sample with high Fe fraction of  $\approx 30\%$ . f) The 3D atom probe analysis for the  $\text{SmCo}_5 + \text{Fe}$  nanocomposite bulk magnet with 60% Fe isoconcentration surface. Panel (b) adapted with permission.<sup>[53]</sup> Copyright 2007, Institute of Physics.

each application to provide the best balance of performance and cost. While the application dictates which performance metrics dominate, in general good soft magnets have the following properties: high saturation magnetization, resistivity, and permeability, and low coercivity and core losses. Operation at elevated temperatures requires a high Curie temperature. Of these parameters, the ones most closely tracked for application are core losses (as a function of maximum applied induction and frequency) and saturation magnetization. Representative values for select soft magnetic alloys are shown in Table 6. Graphically, the classes of soft magnetic materials are defined in Figure 3 with the bounds of saturation magnetization and coercivity values shown.

Since the origin of core losses is strongly dependent on the choice of material, the materials selection can result in very different optimal component designs. Figure 18 shows the core losses for selected soft magnetic materials as a function of the maximum flux density and using a sinusoidal switching field at 50 or 60 Hz. The amorphous (e.g., Metglas) and nanocrystalline (e.g., Finemet) alloys provide the greatest energy efficiency with the lowest core losses for a given applied magnetic field (or flux density) and frequency (not shown). This is largely due to their low values of magnetocrystalline anisotropy, which determines the resistance of domain wall motion through the material when a magnetic field is applied. The coercivity is a parameter from Table 6 that reflects the low value of magnetocrystalline anisotropy and is proportional to the hysteretic losses in the material (a component of the total core losses). Amorphous and nanocrystalline alloys have the added benefit of moderate resistivity, which limits the effects of eddy currents on the total core losses allowing them to be used at higher switching

frequencies. These advanced classes of alloys provide flexibility in device design.

Most transformers are designed for optimal energy efficiency, splitting the losses of the system between those generated by the core and those generated by the copper windings (Figure 19). This is done to transfer the maximum amount of power per core volume and to keep the rise in the temperature of the core to a minimum. The resulting design shows that the lowest total losses are coincident with an optimal flux density change for the transformer. The position of the optimal flux density is dependent on the core material and number of turns on the transformer. The saturation of the magnetization of the core material provides an upper limit to the flux density change (although in practice the maximum useful flux density is considerably lower due to reduced permeability of the core as a near saturating field is applied).

While utility transformers tend to have high efficiency (above  $\approx 97\%$ ), their ubiquitous use means that even small improvements in core loss can have large energy savings systemically. Electrical steels (e.g., Fe 3%Si) are typically used in utility transformers due to their low cost and high magnetization. However, their core losses are substantially higher than recently developed nanocrystalline materials.<sup>[65]</sup> The move to high-energy-efficiency magnetic cores requires a larger initial capital investment however a significant reduction in no-load losses, almost entirely due to the magnetic material, provides a cost savings over the lifetime of the transformer due to the improved efficiency.<sup>[66]</sup> Higher efficiency also results in reduction of  $\text{CO}_2$  emission since less electrical energy is wasted in the transmission and distribution process.<sup>[67]</sup> Conversion technologies for wind, solar, and storage by flywheel technology (i.e., off-peak energy storage of electricity generated by wind and solar technologies) will also require magnetic converters to change the solar or wind directly (or the stored mechanical energy in the flywheel) to electrical energy.<sup>[68]</sup>

Improvements in transportation technologies will also demand advanced soft magnetic materials. As hybrid electric and battery electric vehicles are developed and produced in increasing numbers, the need for miniaturized, high efficiency advanced induction motors and power converters to charge these vehicles will require advances in materials. In this case, large magnetization and higher frequency operation will allow miniaturization of the motors and generators, providing better efficiency for the system. Elevated temperature power generation and conversion will be necessary for electric aircraft and ships, as well as improved efficiency at higher operation frequencies for power electronics devices. Switch-mode power supplies used in power electronics applications require materials with a square magnetic hysteresis loop and low AC losses for magnetic amplification purposes as well as a broadband high permeability core to smooth out the ripple current.<sup>[69]</sup> As distributed power sources become more widespread, the necessity for DC/DC conversion of large output currents will require advanced core materials to operate efficiently at low voltages

**Table 6.** Magnetic properties for various commonly used soft magnetic materials.<sup>[60–62]</sup> Note: the Metglas alloy is amorphous and the Finemet alloy is nanocrystalline. One Tesla exceeds the saturation magnetization for alloys marked with †.

| Material   | $\mu_0 M_s$ (T) | $\mu_{max}$ ( $10^3$ ) | $H_c$ (A/m) | electrical resistivity ( $\rho_e$ ) ( $\mu\Omega\text{cm}$ ) | $T_c$ ( $^\circ\text{C}$ ) | $P_{cm}$ [60 Hz/1 T] (W/kg) | magnetostriction ( $\lambda_s$ ) (ppm) |
|--|-----------------|------------------------|-------------|--|----------------------------|-----------------------------|--|
| $\text{Fe}_{49}\text{Co}_{49}\text{V}_2$                                   | 2.4             | 5–50                   | 16–398      | 27   | 930                        | 1.10                        | 60                                     |
| Soft Fe  | 2.16            | 10–50                  | 4–80        | 10   | 771                        | 20                          | –2                                     |
| Fe 3%Si (GO)   | 2.0             | 0.5–5                  | 6           | 48   | 745                        | 0.84                        | 7                                      |
| $\text{Fe}_{67}\text{Co}_{18}\text{B}_{14}\text{Si}_1$                     | 1.8             | 50                     | 3.5         | 123  | 415                        | 0.66                        | 35                                     |
| Metglas 2605CO   |                 |                        |             |  |                            |                             |  |
| $\text{Ni}_{50}\text{Fe}_{50}$ permalloy                                   | 1.4–1.6         | 70                     | 4–20        | 40–50  | 480                        | 0.33                        | 18                                     |
| $\text{Fe}_{73.5}\text{Si}_{13.5}\text{Nb}_3\text{B}_9\text{Cu}_1$ Finemet | 1.23–1.35       | 80                     | 0.6–2.5     | 110  | 570                        | 0.01                        | 0–2                                    |
| $\text{Ni}_{78}\text{Fe}_{17}\text{Mo}_5$ supermalloy                      | 0.65–0.82       | 100–800                | 0.25–0.64   | 60   | 400                        | †                           | 2–3                                    |
| Mn-Zn ferrite  | 0.36–0.5        | 0.5–10                 | 10–100      | $10^7$ – $10^8$  | 150–250                    | †                           | $\pm 5$                                |
| Ni-Zn ferrite  | 0.25–0.42       | 0.01–1                 | 14–1600     | $10^{11}$  | 120–500                    | †                           | –20                                    |

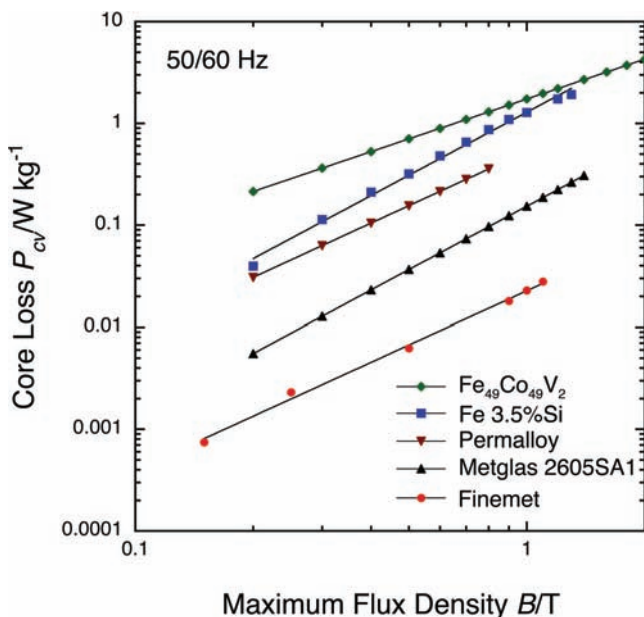
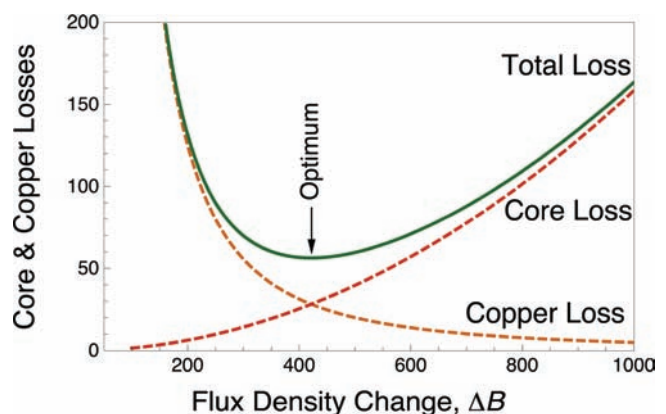
and high frequencies (in conjunction with a move to GaAs or SiC semiconductor active components).

Size and weight reductions can be achieved for a given output power requirement by increasing the operation frequency, as demonstrated in the schematic diagram from **Figure 20**.<sup>[70,71]</sup> For instance, for a 500 W output power the volume of the transformer can be reduced by 50% when the frequency is raised from 6 to 60 kHz. As size and weight are extremely important for transportation applications (including electric and hybrid cars and ships), exploitation of this effect would be very advantageous, however, the losses of the system are not represented in this figure, and both the core and copper losses increase with increasing frequency. Recent improvement in soft magnetic performance by microstructure and composition

control have been active areas of research to provide more material options for better energy efficiency at higher operation frequencies.<sup>[72,73]</sup>

Great improvements in energy efficiency have been demonstrated for amorphous and nanocrystalline soft magnetic materials. Due to the higher capital costs, this technology has not received wide-spread use despite the availability of promising materials research during the past 20 years, and the lower life-cycle cost of using these cores.<sup>[66]</sup> The use of amorphous alloys has been shown to reduce transformer size and reduce acoustic noise when compared to conventional Si-steels used in most transformer cores today. Additionally, the improved energy efficiency of transformers using these materials results in reduced carbon emissions considering the majority of electricity is generated from fossil fuels.

While recent soft magnetic materials developments have resulted in advances in low-loss magnetic alloys, many of these developments require sustained research investment to improve the magnetization, magnetostriction, and extend their upper operation frequency. Investment in the development of

**Figure 18.** Core loss as a function of maximum flux density for various soft magnetic materials with a 50 or 60 Hz switching field.<sup>[62–64]</sup>**Figure 19.** Schematic diagram showing the contributions of copper and core losses used in transformer design with the most energy efficient design indicated as optimum.

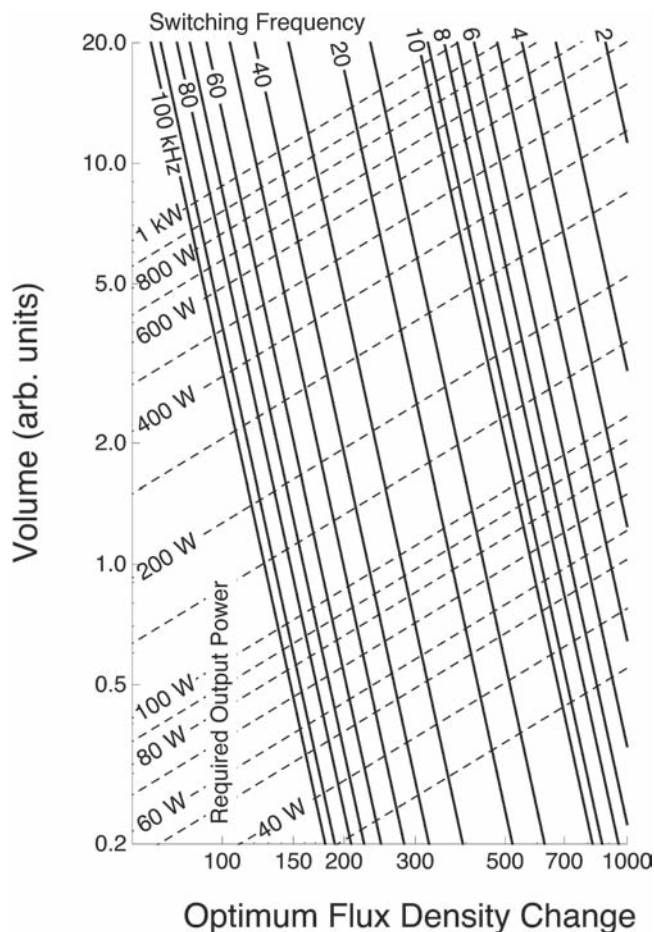


**Figure 20.** Schematic diagram showing the relationship between required power output, switching frequency, and volume as a function of optimum changes in flux density for a model switchmode transformer.

high-efficiency soft magnetic materials now will enable more flexible engineering designs for electronics and transportation to meet tomorrow's energy needs.

#### 4. Magnetocaloric Materials

Modern society relies on readily available refrigeration for protecting food and providing comfortable living spaces. Conventional refrigerators use ozone depleting chemicals (chlorofluorocarbons (CFCs)), hazardous chemicals (ammonia (NH<sub>3</sub>)), or greenhouse gases (hydrochlorofluorocarbons (HCFCs) and hydrofluorocarbons (HFCs)) in a vapor-compression cycle to provide cooling. While they have met the cooling needs and improved the standard of living for people worldwide, conventional refrigerators tend to be unwieldy, hefty, and lack energy efficiency. Recently, an alternative refrigeration method using adiabatic demagnetization (the so-called magnetocaloric effect (MCE)) has been investigated as a means to address the short-comings of vapor-compression refrigeration. Magnetic refrigeration has three prominent advantages compared to compressor-based refrigeration. First there are no

harmful gasses involved, second it may be built more compactly because the main working material is a solid, and third magnetic refrigerators generate much less noise. Also, the cooling efficiency in magnetic refrigerators working with gadolinium has been shown to reach 60% of the theoretical limit,<sup>[74]</sup> compared to only about 45% in the best gas-compression refrigerators. While commercial refrigerators of this type are still in the development stages, research efforts to develop new materials with improved MCE are focused on maximizing the cooling capacity and energy efficiency of this budding technology. In this section, the different materials are compared, concentrating on transition metal containing compounds.

When a material is magnetized in an applied magnetic field, the entropy associated with the magnetic degrees of freedom, the so-called magnetic entropy,  $S_m$ , is changed because the field changes the magnetic order of the material. Under adiabatic conditions,  $\Delta S_m$  must be compensated by an equal but opposite change in the entropy associated with the lattice, resulting in a change in the temperature of the material. This temperature change,  $\Delta T_{ad}$ , is usually called the MCE. It is related to the magnetic properties of the material through the thermodynamic Maxwell relation  $(\frac{\partial S}{\partial B})_T = (\frac{\partial M}{\partial T})_B$ . From magnetization measurements made at discrete temperature intervals,  $\Delta S_m$  can be calculated as described in Refs. [75,76]. For materials showing a first-order phase transition with large hysteresis these magnetization measurements need to be done with great care to avoid overestimation of the entropy change.<sup>[77]</sup> On the other hand, the magnetic entropy change can be obtained more directly from a calorimetric measurement of the field dependence of the heat capacity,  $c$ , and subsequent integration. It has been confirmed that the values of  $\Delta S_m(T,B)$  derived from the magnetization measurement coincide with the values from calorimetric measurement.<sup>[78]</sup> The adiabatic temperature change,  $\Delta T_{ad}(T,B)$ , can then be integrated numerically using the experimentally measured or theoretically predicted magnetization and heat capacity. Obviously, the MCE is large when  $(\frac{\partial M}{\partial T})_B$  is large and  $c(T,B)$  is small at the same temperature. As we are interested in effects at higher temperatures, the heat capacity is generally quite large, on the order of the Dulong–Petit law,  $c \approx 3NR$ , where  $N$  is the number of atoms and  $R$  is the molar gas constant. Therefore, we should concentrate on finding a large change in magnetization at the relevant temperature. Since  $(\frac{\partial M}{\partial T})_B$  peaks at the magnetic-ordering temperature, a large MCE is expected close to this magnetic phase transition and the effect may be further maximized, when the order parameter of the phase transition changes strongly within a narrow temperature interval. The latter is true for first-order phase transitions.

In the magnetic-refrigeration cycle, depicted in **Figure 21**,<sup>[79,80]</sup> initially randomly oriented magnetic moments are aligned by a magnetic field, resulting in heating of the magnetocaloric material. This heat is removed from the material to the ambient environment by heat transfer. Upon removing the field, the magnetic moments randomize, which leads to cooling of the material below ambient temperature. Heat from the system to be cooled can then be extracted using a heat-transfer medium. Depending on the operating temperature, the heat-transfer medium may be water (with antifreeze) or air and, for very low temperatures, helium. Therefore, magnetic refrigeration is an environmentally friendly cooling technology. Current research aims at new magnetic

materials with larger magnetocaloric effects, which then can be operated in fields of about 2 T or less (i.e., fields that can be generated by the aforementioned Nd-Fe-B-type permanent magnets).

#### 4.1. La(Fe,Si)<sub>13</sub> and Related Compounds

The Fe-rich compounds La(Fe,Si)<sub>13</sub>, with the cubic NaZn<sub>13</sub>-type structure, possess magnetic ordering temperatures between 200 and 262 K and exhibit typical invar-type behavior.<sup>[81,82]</sup> Due to the sharp first-order magnetic-ordering transition, several groups have reported a large magnetocaloric effect for this class of compounds,<sup>[83,84]</sup> which is enhanced when the materials are processed by rapid quenching and subsequent annealing.<sup>[85–87]</sup> Above the Curie temperature  $T_c$ , an itinerant-electron metamagnetic (IEM) transition is induced by an external magnetic field. The IEM transition occurs due to the change in the density of states at the Fermi level under the action of the magnetic field. Both transitions to the ferromagnetic state are accompanied by a sizable volume change of about 1%.<sup>[88]</sup> In real materials, the lattice parameter can be modified physically by applying external pressure or chemically by the addition of substitutional or interstitial alloying elements.<sup>[89]</sup> To increase the magnetic-ordering temperature without significant loss in the magnetic moment, one may replace some Fe by other magnetic transition metals. The compounds La(Fe,Co)<sub>13–x</sub>Al<sub>x</sub> and La(Fe,Co)<sub>13–x</sub>Si<sub>x</sub> with  $x \approx 1.1$  and therefore a very high transition metal content show a considerable magnetocaloric effect near room temperature.<sup>[90,91]</sup> This is achieved with only a few percent of Co and the Co content can easily be varied to tune the critical temperature to the desired value, however, near room temperature the values for the entropy drop.

Further improvement in the magnetocaloric effect can be achieved by expanding the crystalline lattice, thereby influencing the character of the direct exchange interaction (from

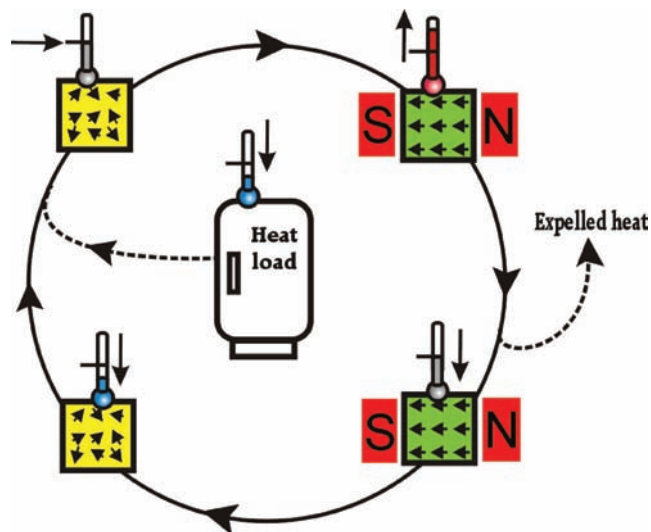


**Figure 21.** Schematic representation of a magnetic-refrigeration cycle that transports heat from the heat load to the ambient environment. Yellow and green depict materials in low and high magnetic fields, respectively. Reproduced with permission.<sup>[80]</sup> Copyright 2005, Institute of Physics.

antiferromagnetic to ferromagnetic). The lattice expansion due to the addition of three interstitial hydrogen atoms per formula unit is about 1.5%.<sup>[92–94]</sup> The critical temperature can be increased to up to 450 K, the average magnetic moment per Fe increases from 2.0  $\mu_B$  to up to 2.2  $\mu_B$  and the field- or temperature-induced phase transition is found to be of first-order for all hydrogen concentrations. This all results for a certain Si percentage in an almost constant value of the magnetic entropy change per mass unit over a broad temperature range (Figure 22).

Material processing will be somewhat more elaborate than for simple metal alloys, however La is the cheapest of the rare-earth elements so these materials should be cost-effective. Due to the above described changes in lattice parameters caused by the phase transitions and/or hydrogenation, the material will potentially have long-term cycling problems because the polycrystalline material may become granular with use. This can have distinct influence on the corrosion resistance of the material and thus on the lifetime of a refrigerator and therefore must be investigated. Very recently, it could be demonstrated that powderized bulk materials and melt-spun particles can be hot-compacted to a porous morphology. The porous structure is much more tolerant to the huge magnetoelastic effects related to the first-order-type transitions and retains their mechanical integrity over hundreds of cycles.<sup>[96]</sup> Only a slight decrease in the adiabatic temperature change compared to the conventional bulk material was observed and, with this, one of the major obstacles for application can be regarded as being overcome.

#### 4.2. MnAs-Based Compounds

MnAs exists in two distinct crystallographic structures.<sup>[97]</sup> At low- and high-temperature the hexagonal NiAs structure is found and for a narrow temperature range from 307 to 393 K the orthorhombic MnP structure exists. The high-temperature transition in the paramagnetic region is of second-order. The low-temperature transition is a combined structural and ferro-paramagnetic transition of first-order with large thermal

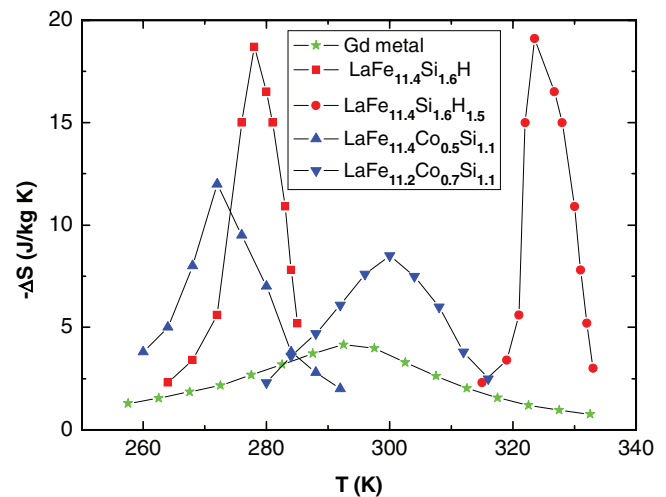


**Figure 22.** Magnetic entropy change for different LaFe<sub>13</sub>-based samples at a field change of 2 T.<sup>[92,95]</sup>

hysteresis. The change in volume at this transition amounts to 2.2%.<sup>[98]</sup> The transition from paramagnetic to ferromagnetic occurs at 307 K, the reverse transition from ferromagnetic to paramagnetic occurs at 317 K. Very large magnetic entropy changes are observed in this transition.<sup>[99]</sup> In the concentration range from 5 to 40% Sb,  $T_C$  can be tuned between 220 and 320 K without losing much of the magnetic entropy change.<sup>[100]</sup> Direct measurements of the temperature change confirm a  $\Delta T$  of 2 K  $T^{-1}$ .<sup>[101]</sup> When Mn is substituted by Cr the thermal hysteresis is reduced and  $T_C$  is lowered, while the large entropy change is maintained.<sup>[102]</sup>

The materials costs of MnAs are quite low but processing of As containing alloys is complicated due to the biological activity of As. In the MnAs alloy the As is covalently bound to the Mn and would not be easily released into the environment. However, this should be experimentally verified, in particular because in an alloy second phases frequently form and may be less stable. The change in volume in MnAs and MnSb is still 0.7% which may result in aging after frequent cycling of the material.

#### 4.3. Heusler Alloys

Heusler alloys frequently undergo a diffusionless, displacive or martensitic transformation between austenite, a high temperature, cubic, parent phase, and martensite, a low temperature, tetragonal phase. The transformation is generally temperature-induced and of first-order. While this effect has been carefully considered for magnetic shape memory applications,<sup>[103]</sup> it may also be exploited for magnetic refrigeration. Very close to the martensitic-transition temperature, one observes a large change in magnetization for low applied magnetic fields due to the change in magnetocrystalline anisotropy between the austenite and martensite phases. This change in magnetization can result in a moderate MCE.

An example of a material from this class with good magnetocaloric response is  $Ni_2MnGa$ , which has a ferromagnetic Curie temperature of 376 K and a martensitic-transformation temperature near 220 K.<sup>[104]</sup> This martensitic-transformation temperature can be easily changed to around room temperature by modifying the composition of the alloy from the stoichiometric one. As may be expected from its cubic structure, the parent phase has a low magnetocrystalline anisotropy ( $\mu_0 H_a = 0.15$  T). However, the martensitic phase exhibits a much larger anisotropy ( $\mu_0 H_a = 0.8$  T). The corresponding changes in the response to an applied magnetic field during the transformation results in a moderate magnetic entropy change of a few  $J mol^{-1} K^{-1}$  (Figure 23), which is enhanced when measured on a single crystal.<sup>[105,106]</sup> When the composition in this material is tuned in a way that the magnetic and structural transformation occurs at the same temperature, the largest magnetic-entropy changes are observed.<sup>[107]</sup>

Some of Heusler alloys with In or Sn as the p-metal show an inverse MCE. These materials cool down upon application of a magnetic field.<sup>[110–112]</sup> This effect is related to the difference in exchange interaction for the austenitic and martensitic phase and may be useful for special applications. A detrimental feature of the martensitic transition, the rather large thermal hysteresis, can to some extent be controlled by either composition, processing,<sup>[113]</sup> or hydrostatic pressure.<sup>[114]</sup> Additionally,

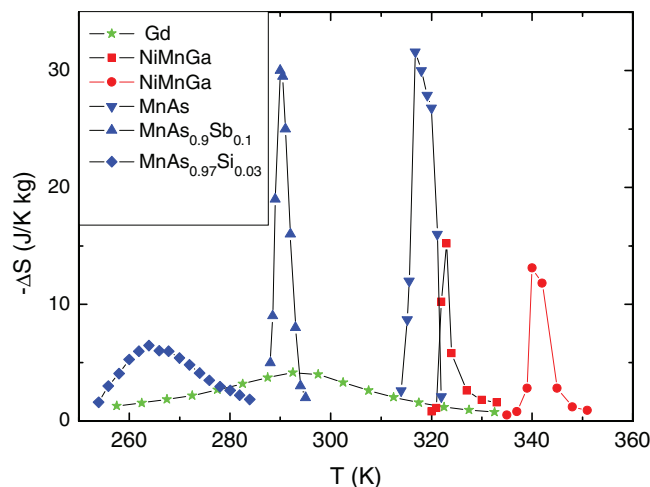


**Figure 23.** Magnetic-entropy change for MnAs and  $Mn_{1+\delta}As_{0.9}Sb_{0.1}$ ,<sup>[100]</sup>  $MnAs_{0.97}Si_{0.03}$ ,<sup>[108]</sup> and two  $NiMnGa$ <sup>[109]</sup> alloys at a field change of 2 T.

the extremely large length changes related to the martensitic transition will definitely result in aging effects. It is well-known for the magnetic shape memory (MSM) alloys that only single crystals can be frequently cycled and polycrystalline materials spontaneously powderize after several cycles. The synthesis of polymer-composite MSM materials does circumvent this effect.<sup>[115,116]</sup>

#### 4.4. $Fe_2P$ -Based Compounds

Another phenomenon leading to a large MCE is the discontinuous volume change that accompanies the magnetic transition observed in  $Fe_2P$ -type alloys with Mn and As substitutions. The Curie temperature of this compound is 216 K and the magnetic transition is of first-order.<sup>[117]</sup> The magnetic-ordering transition from the paramagnetic state to the ferromagnetic state is accompanied by a discontinuous change in the volume of 0.05%. Thus, the ferromagnetic state has a higher volume than the paramagnetic one. This phase transition is found to be extremely sensitive to changes in pressure or magnetic field. Substitution of As, B, or Si into the P sublattice results in an increase of the Curie temperature, which can easily be lifted to above room temperature for As or Si concentrations of 10% or B concentrations of 4%.<sup>[118]</sup>

The most extensively studied series of alloys is of the type MnFe, MnP, and MnAs. The most striking feature of the MnFeP–MnFeAs phase diagram is the stability of the hexagonal  $Fe_2P$ -type structure for As concentrations between 30 and 65%.<sup>[119]</sup> This phase has ferromagnetic order accompanied by a discontinuous change in volume and a resultant large magnetocaloric effect.<sup>[120–122]</sup> While the total magnetic moment is not affected by changes in the composition, the Curie temperature can be tuned from 200 to 450 K.

For these compounds one observes a strong change in the critical temperature on the application of a magnetic field. This change in critical temperature is a good indication for the temperature change induced by the application of a magnetic field.<sup>[123]</sup> The thermal hysteresis is signature of a first-order

phase transition. Because of the small size of the thermal hysteresis (less than 1 K), the magnetization process can be considered to be reversible in temperature. Variation of the Mn:Fe ratio may also be used to further improve the MCE. More recently, a large MCE was observed in the compound  $\text{MnFeP}_{0.5}\text{As}_{0.3}\text{Si}_{0.2}$  at room temperature (see Figure 24).<sup>[124]</sup> After replacing all As, a considerable large MCE is still observed for MnFe, MnP, MnSi, and MnGe.<sup>[125,126]</sup> However, these alloys exhibit a much larger thermal hysteresis. Processing and variation of the stoichiometry on the transition-metal sublattice appear to help avoid the undesired hysteresis.<sup>[127,128]</sup>

The excellent magnetocaloric features of the compounds of the type MnFe, MnP, MnSi, MnGe, and MnAs and the very low material costs make them attractive candidate materials for commercial magnetic refrigerators. However, as is the case for MnAs alloys it should be verified that materials containing As do not release this to the environment. The fact that the magnetoelastic phase transition is a change of the lattice parameters rather than a change in volume makes it feasible that this alloy, even in polycrystalline form, will not experience severe aging effects after frequent magnetic cycling.

#### 4.5. Comparison of Different Materials and Outlook

The MCEs for field changes of 2 T are summarized in Figure 25. It is obvious that above room temperature a few transition-metal-based alloys perform the best. If one takes into account the fact that  $\Delta T$  also depends on the specific heat of the compound<sup>[129]</sup> these alloys are still favorable and not only from the cost point-of-view. This makes them likely candidates for use as magnetic refrigerant materials above room temperature. However, below room temperature a number of rare-earth compounds perform better and for these materials a thorough cost versus performance analysis will be needed.

The main parameters of the various materials are also summarized in Table 7, permitting a fast comparison. At present it is not clear which material will get to the stage of real life applications. Though it is already feasible that for applications with limited temperature span and a cooling power in the kW range like air conditioning, commercial competitive magnetic refrigerators are quite possible, it is not yet obvious, which of the above mentioned materials shall be employed. A variety of prototypes have been built<sup>[130,131]</sup> but materials are not yet available at large scale. Though most attention is paid to the

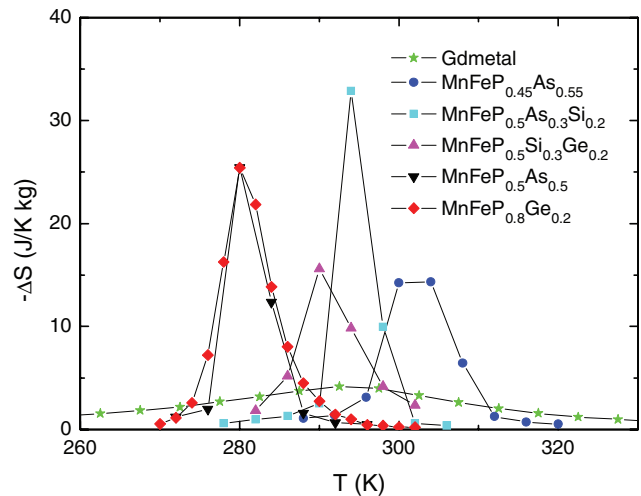


Figure 24. Magnetic-entropy changes of  $\text{Fe}_2\text{P}$  type compounds at magnetic field changes of 2 T.<sup>[120–122]</sup>

pure magnetocaloric properties and materials costs, recently also other properties like dynamics of the phase transition,<sup>[132]</sup> corrosion resistance, mechanical properties, heat conductivity, electrical resistivity and environmental impact are getting attention. With the refrigeration market being a multibillion dollar market, this novel technology offers great opportunities.

Taking into account the different requirements for magnetic refrigerants, it may be stated that the ideal magnetic refrigerant should at least contain 80% transition metals with a large magnetic moment such as Fe or Mn. In addition it should contain some inexpensive p-metal such as Al or Si, which can be used to tune the working point of the material. This material should then exhibit a magnetic ordering transition of first-order and be as workable as steel, with a corrosion resistance similar to stainless steel and a high electrical resistance.

## 5. Summary

In this review we have described an existing but somehow largely ignored fact that improved magnetic materials are a solution to the energy crisis. The solution via development in magnetic materials will give an immediate impact in producing renewable energy and in raising energy efficiency. Magnetic materials have already played a significant role in energy

Table 7. Comparison of different potential magnetocaloric materials. Gd is included as reference material ([d] means direct measurement, [c] is calculated from a combination of measurements). The costs may strongly fluctuate due to market demands and quality of starting materials. Reproduced with permission.<sup>[80]</sup> Copyright 2005, Institute of Physics.

| Material                                 | T range (K) | $\Delta S_{\text{max}}$ (2T) ( $\text{J kg}^{-1} \text{K}^{-1}$ ) | $\Delta T$ (2T) (K) | $T_{\text{C}}$ (K) | Cost €/kg | Density ( $\times 10^3 \text{ kg m}^{-3}$ ) | Ref.    |
|--|-------------|---|---------------------|--------------------|-----------|---|---------|
| Gd                                       | 270–310     | 5   | 5.8 <sup>[d]</sup>  | 293                | 20        | 7.9   | [79]    |
| $\text{Gd}_2\text{Ge}_2\text{Si}_2$      | 150–290     | 27  | 6.6 <sup>[d]</sup>  | 272                | 60        | 7.5   | [134]   |
| $\text{La}(\text{Fe},\text{Si})\text{H}$ | 180–350     | 19  | 7 <sup>[c]</sup>    | 300                | 8         | 7.1   | [87,88] |
| MnAs                                     | 220–320     | 32  | 4.1 <sup>[d]</sup>  | 287                | 10        | 6.8   | [101]   |
| MnNiGa                                   | 310–350     | 15  | 2 <sup>[c]</sup>    | 317                | 10        | 8.2   | [116]   |
| MnFe(P,As)                               | 150–450     | 32  | 6 <sup>[d]</sup>    | 292                | 7         | 7.4   | [134]   |

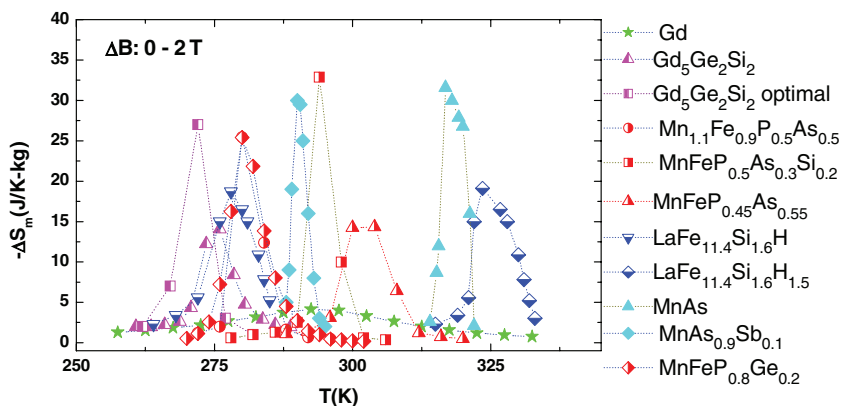


Figure 25. Magnetic-entropy change of different materials at magnetic field changes of 2 T. Reproduced with permission.<sup>[80]</sup> Copyright 2005, Institute of Physics.

applications and improved and innovated magnetic materials will play an even more important role in energy solutions. They contribute to saving electric power and reducing CO<sub>2</sub> emissions in multiple ways. For example, the conversion of electrical energy into mechanical work and vice versa is done using electric motors and generators, respectively, which imply the use of hard and soft magnetic materials. Permanent magnets play an essential role in improving the efficiency of electricity transmission and utilization and also in the progressive replacement of oil-based fuels in transportation by electric motors. For electric vehicles, magnetic materials must retain their properties up to moderately high temperatures, which is demanding for most of the materials currently in use. Thus, optimizing soft and hard magnetic materials and extending the temperature span in which they are applicable implies a notable enhancement in the energy efficiency of these devices.

There are also novel magnetic materials that can help us reach larger energy efficiency. One example is magnetic refrigerants for solid-state energy-efficient cooling. Taking into account that the largest electricity consumption in the domestic market is related to refrigeration and air conditioning, the improvement of these devices via the use of magnetic technologies will translate into a large reduction in energy consumption. Other examples are power-MEMS for energy harvesting and electromagnetic conversion using microfabricated permanent magnets. Here, an electromagnetic vibration-to-electrical power generator can efficiently scavenge energy from low-frequency external vibrations. The generator up-converts low-frequency environmental vibrations to a much higher frequency through an electromechanical frequency up-converter using a magnet and, hence, provides efficient energy conversion even at low frequencies.

While recent progress in magnetic materials developments have resulted in advances in increasing energy density, reducing rare-earth contents, and lowering eddy current losses, many of these developments require sustained research investment to improve the magnetization, temperature stability, and operation frequency. Investment in the development of high-efficiency hard and soft magnetic materials now will enable more flexible engineering designs for electronics and transportation to meet tomorrow's energy needs.

## Acknowledgements

O.G. thanks the DFG, BMBF, EU, and various industrial partners for their financial support in the past twelve years to his research effort in advanced functional magnetic materials. M.A.W. thanks NRL, ONR, and DARPA for financial support to his research effort in magnetic materials. E.B. thanks the STW, FOM, and NWO for financial support. CHC thanks the US Air Force, ARO, DARPA, NASA, and NSF for their support in the past decade to her research effort in magnetic materials and computer simulations. S.G.S. acknowledges several grants and contracts from the US DOE, DARPA, ARO, Naval Air Systems Command, Lakehurst, NJ, and Pennsylvania's DEP. J.P.L. thanks the US/DoD/DARPA, ARO, ONR, NSF, and the University of Texas for their financial support in the past ten years to his research efforts in nanocomposite magnetic materials.

Received: June 14, 2010

Published online: December 15, 2010

- [1] For a thorough discussion on this topic, see "U. S. Adoption of High-Efficiency Motors and Drives: Lessons Learned: M. Lowe, R. Golini, and G. Gereffi, published by Center on Globalization, Governance and Competitiveness (February 2010).
- [2] *International Energy Annual*, U.S. Energy Information Administration, **2006**.
- [3] *Annual Energy Review*, Energy Information Administration, U. S. Department of Energy, **2007**, p. 62.
- [4] *Annual Energy Review*, Tables 2.1(b,f), 2008, pp. 41 and 45.
- [5] K. A. Gschneidner, Jr., V. K. Pecharsky, A. O. Tsokol, *Rep. Prog. Phys.* **2005**, *68*, 1479.
- [6] C.-J. Winter, *Int. J. Hydrogen Energy* **2009**, *34*, S1.
- [7] M. Z. Jacobson, M. A. Delucchi, *Sci. Am.* **2009**, *301*, 58.
- [8] O. Gutfleisch, *J. Phys. D: Appl. Phys.* **2000**, *33*, R157.
- [9] S. Sugimoto, in *Proc. 20th Int. Workshop on Rare Earth Permanent Magnets and their Applications*, (Ed: D. Niarchos), **2008**, 106.
- [10] D. Hinz, J. Lyubina, G. Fuchs, D. N. Brown, B. M. Ma, O. Gutfleisch, K.-H. Müller, *J. Magn. Magn. Mater.* **2004**, *272–276*, e321.
- [11] C. H. Chen, M. H. Walmer, S. Liu, *IEEE Trans. Magn.* **2004**, *40*, 2937.
- [12] O. Gutfleisch, K.-H. Müller, K. Khlopkov, M. Wolf, A. Yan, R. Schäfer, T. Gemming, L. Schultz, *Acta Mater.* **2006**, *54*, 997.
- [13] A. S. Holmes, G. Hong, K. R. Pullen, *J. Microelectromech. Sys.* **2005**, *14*, 54.
- [14] H. Raisigel, O. Cugat, J. Delamare, *Sens. Actuators, A* **2006**, *103–131*, 438.
- [15] S. Das, D. P. Arnold, I. Zana, J. W. Park, J. H. Lang, *IEEE MEMS 2005 Conference*, Miami, USA, **2005**, 287.
- [16] O. Gutfleisch, N. Dempsey, in: *Magnetic Nanostructures in Modern Technology*, (Eds: B. Azzerboni, G. Asti, L. Pareti, M. Ghidini), Springer, Berlin, **2008**, 167.
- [17] N. M. Dempsey, A. Walther, F. May, D. Givord, K. Khlopkov, O. Gutfleisch, *Appl. Phys. Lett.* **2007**, *90*, 092509.
- [18] C. H. Chen, M. S. Walmer, M. H. Walmer, S. Liu, G. E. Kuhl, G. K. Simon, in *Materials Research Society Symposium Proceedings 577*, Advanced Hard and Soft Magnetic Materials, MRS, Warrendale PA **1999**, 277.
- [19] G. C. Hadjipanayis, W. Tang, Y. Zhang, S. T. Chui, J. F. Liu, C. Chen, H. Kronmüller, *IEEE Trans. Magn.* **2000**, *36*, 3382.

- [20] M. S. Walmer, C. H. Chen, M. H. Walmer, *IEEE Trans. Magn.* **2000**, 36, 3376.
- [21] C. H. Chen, *Engineering magnetic materials and their applications, Course MAT-512, University of Dayton*, **2006–2010**.
- [22] Yang Luo, *Proc. 20th Int. Workshop on Rare Earth Permanent Magnets and Their Applications*, (Ed: D. Niarchos), **2008**, 27.
- [23] USMagneticMaterialsAssociation, <http://www.usmagnetmaterials.com/documents/usmma-presentation-general-5-08.ppt>, (accessed September 2010).
- [24] J. F. Herbst, J. J. Croat, F. E. Pinkerton, W. B. Yelon, *Phys. Rev. B* **1984**, 29, 4176.
- [25] D. Kennedy, presented at Materials for Sustainable Energy, Birmingham, UK, September **2009**.
- [26] Metal Pages Homepage, [www.metal-pages.com](http://www.metal-pages.com) (accessed September 2010).
- [27] O. Gutfleisch, I. R. Harris, *J. Phys. D: Appl. Phys.* **1996**, 29, 2255.
- [28] O. Gutfleisch, K. Khlopkov, A. Teresiak, K. H. Müller, G. Drazic, C. Mishima, Y. Honkura, *IEEE Trans. Magn.* **2003**, 39, 2926.
- [29] M. Zakotnik, I. R. Harris, A. J. Williams, *J. Alloys Compd.* **2008**, 450, 525.
- [30] I. R. Harris, J. P. McGuinness, D. G. R. Jones, J. S. Abell, *Phys. Scr.* **1987**, 19, 435.
- [31] J. F. Gieras, M. Wing, *Permanent Magnet Motor Technology Design and Applications*, Marcel Dekker, N. Y., USA **2002**.
- [32] *Handbook of Small Electric Motors*, (Eds: W. H. Yeadon, A. W. Yeadon), McGraw-Hill, New York **2001**.
- [33] Jun Kang, *General Purpose Permanent Magnet Motor Drive without Speed and Position Sensor*, Yaskawa Electric Corp., Japan, Yaskawa Application Note WP.AFD.05.pdf, [http://www.yaskawa.com/site/dmdrive.nsf/link2/NKOE-7U9HJG/\\$file/WP.AFD.05.pdf](http://www.yaskawa.com/site/dmdrive.nsf/link2/NKOE-7U9HJG/$file/WP.AFD.05.pdf) (accessed September 2010).
- [34] Y. Honkura, *Proc. of 19th Int. Workshop on Rare Earth Permanent Magnets and Their Applications*, *J. Iron Steel Res. Int.* **2006**, 13, 231.
- [35] S. Simizu, F. Pourarian, W. E. Wallace, *Proc. 11th Int. Workshop on Rare Earth Magnets and Their Applications*, (Ed: S. G. Sankar), Carnegie Mellon University, Pittsburgh PA **1990**, 191.
- [36] World Wind Energy Association, <http://www.wwindea.org>, report from March 2010.
- [37] H. Polinder, F. F. A. Van Der Pijl, G. J. de Vilder, P. Tavner, *IEEE Trans. Energy Conversion* **2006**, 21, 725.
- [38] S. Makaremi, *Clipper's design approach to improving reliability*, <http://www.sandia.gov/wind/2007ReliabilityWorkshopPDFs/Mon-11-ShawMakaremi.pdf> (accessed September 2010).
- [39] G. Bywaters, V. John, J. Lynch, P. Mattila, G. Norton, J. Stowell, M. Salata, O. Labath, A. Chertok, D. Hablanian, *Northern Power Systems Wind PACT Drive Train Alternative Design Study Report (2005)*, National Renewable Energy Laboratory, <http://www.nrel.gov/docs/fy05osti/35524.pdf>, (accessed September 2010).
- [40] E. de Vries, *Renewable Energy World Int. Magazine* **13**, **2010**.
- [41] Clipper Windpower, [http://www.clipperwind.com/pdf/liberty\\_brochure.pdf](http://www.clipperwind.com/pdf/liberty_brochure.pdf) (accessed September 2010).
- [42] Henri Pieper, *Regelungsvorrichtung für mit Dynamomaschinen gekuppelte Explosionskraftmaschinen*, Patentschrift Nr. 21202, Kais. Königl. Österreichische Patentamt, **1905** (Pieper first submitted the German version in 1905 and four years later the US patent).
- [43] Toyota Motor Corporation, Public Affairs Division, "TOYOTA HYBRID SYSTEM", May 2003.
- [44] C. C. Chan, *Proc. IEEE* **2002**, 90, 247.
- [45] C. H. Chen, personal communication (**2009**).
- [46] C. Cossar, M. Popescu, T. J. E. Miller, M. McGilp, M. Olaru, *IEEE Trans. Ind. Appl.* **2008**, 44, 1210.
- [47] K. Hirota, T. Ohashi, N. Nakamura, T. Minowa, M. Honshima, *Proc. of 20th Int. Workshop on Rare Earth Permanent Magnets and their Applications*, (Ed: D. Niarchos), **2008**, 122.
- [48] W. F. Brown, *Rev. Mod. Phys.* **1945**, 17, 15.
- [49] W. F. Li, T. Ohkubo, K. Hono, *Acta Mater.* **2009**, 57, 1337.
- [50] J. P. Liu, in *Nanoscale magnetic materials and applications*, (Ed: J. P. Liu, O. Gutfleisch, E. Fullerton, D. Sellmyer), Springer, New York **2009**, p. 309.
- [51] E. F. Kneller, R. Hawig, *IEEE Trans. Magn.* **1991**, 27, 3588.
- [52] V. M. Chakka, B. Altuncevahir, Z. Q. Jin, Y. Li, J. P. Liu, *J. Appl. Phys.* **2006**, 99, 08E912.
- [53] Y. P. Wang, Y. Li, C. B. Rong, J. P. Liu, *Nanotechnology* **2007**, 18, 465701.
- [54] C. B. Rong, Y. Zhang, N. Poudyal, X. Y. Xiong, M. J. Kramer, J. P. Liu, *Appl. Phys. Lett.* **2010**, 96, 102513.
- [55] *Grid 2030 – A National Vision for Electricity's Second 100 Years*, Office of Electric Transmission and Distribution, U. S. Department of Energy, July **2003**.
- [56] *The Smart Grid: An Introduction*, Litos Strategic Communication under DOE contract DE-AC26 – 04NT41817, [www.oe.energy.gov/DocumentsandMedia/DOE\\_SG\\_Book\\_Single\\_Pages\(1\).pdf](http://www.oe.energy.gov/DocumentsandMedia/DOE_SG_Book_Single_Pages(1).pdf) (accessed September 2010).
- [57] Z. Chen, F. Blaabjerg, *Renewable and Sustainable Energy Reviews* **2009**, 13, 1288.
- [58] G. M. J. Herbert, S. Iniyar, E. Sreevalsan, S. Rajapandian, *Renewable Sustainable Energy Rev.* **2007**, 11, 1117.
- [59] *Annual Energy Review*, Energy Information Administration, U. S. Department of Energy, 2007, p. 62.
- [60] C.-W. Chen, *Magnetism and Metallurgy of Soft Magnetic Materials*, Dover Publications, New York **1986**.
- [61] R. C. O'Handley, *Modern Magnetic Materials: Principles and Applications*, John Wiley & Sons, New York **2000**.
- [62] Metglas Inc., *Alloy Specification Sheets*.
- [63] W. Shen, *PhD Thesis*, Virginia Polytechnic Institute and State University, **2006**.
- [64] T. McLyman, *Magnetic Core Selection for Transformers and Inductors*, 2nd Ed., Marcel Dekker, Inc., New York **1997**.
- [65] M. E. McHenry, M. A. Willard, D. E. Laughlin, *Prog. Mater. Sci.* **1999**, 44, 291.
- [66] R. Hasegawa, D. Azuma, *J. Magn. Magn. Mater.* **2008**, 320, 2451.
- [67] R. Hasegawa, *J. Magn. Magn. Mater.* **2000**, 215–216, 240.
- [68] I. Hadjipaschalis, A. Poullikkas, V. Efthimiou, *Renewable Sustainable Energy Rev.* **2009**, 13, 1513.
- [69] R. Hasegawa, *J. Non-Cryst. Solids.* **2001**, 287, 405.
- [70] K. Billings, *Power Electron. Technol.*, June **2004**, p. 56.
- [71] W. G. Hurley, W. H. Wolffe, J. G. Breslin, *IEEE Trans. Power Elect.* **1998**, 13, 651.
- [72] K. E. Knippling, M. Daniil, M. A. Willard, *Appl. Phys. Lett.* **2009**, 95, 222516.
- [73] M. A. Willard, M. Daniil, in *Nanoscale Magnetic Materials and Applications*, (Ed: J. P. Liu, O. Gutfleisch, E. Fullerton, D. Sellmyer), Springer, New York, **2009**, 373.
- [74] C. Zimm, A. Jastrab, A. Sternberg, V. Pecharsky, K. Geschneidner Jr, *Adv. Cryog. Eng.* **1998**, 43, 1759.
- [75] A. M. Tishin, Y. I. Spichkin, *The Magnetocaloric Effect and Its Applications*, Institute of Physics, Bristol, **2003**.
- [76] E. Brück, in *Handbook of Magnetic Materials*, vol. 17, (Ed: K. H. J. Buschow), Publ. North-Holland, Amsterdam, **2008**, p. 235.
- [77] L. Caron, Z. Q. Ou, T. T. Nguyen, D. T. C. Thanh, O. Tegus, E. Bruck, *J. Magn. Magn. Mater.* **2009**, 321, 3559.
- [78] K. A. Gschneidner, V. K. Pecharsky, A. O. Pecharsky, C. B. Zimm, *Rare Earths '98*, **1999**, 315–3, 69.
- [79] O. Tegus, E. Brück, K. H. J. Buschow, F. R. de Boer, *Nature* **2002**, 415, 150.
- [80] E. Brück, *J. Phys. D: Appl. Phys.* **2005**, 38, R381.
- [81] P. I. Kripyakevich, O. S. Zarechnyuk, E. I. Gladyshevsky, O. I. Bodak, *Z. Anorg. Chem.* **1968**, 358, 90.

- [82] M. Palstra, J. A. Mydosh, G. J. Nieuwenhuys, A. M. Van Der Kraan, K. H. J. Buschow, *J. Magn. Magn. Mater.* **1983**, 36, 290.
- [83] F. X. Hu, B. G. Shen, J. R. Sun, X. X. Zhang, *Chin. Phys.* **2000**, 9, 550.
- [84] S. Fujieda, A. Fujita, K. Fukamichi, *Appl. Phys. Lett.* **2002**, 81, 1276.
- [85] O. Gutfleisch, A. Yan, K.-H. Müller, *J. Appl. Phys.* **2005**, 97, 10M305.
- [86] X. B. Liu, X. D. Liu, Z. Altounian, G. H. Tu, *J. Alloys Compd.* **2005**, 397, 120.
- [87] J. Lyubina, O. Gutfleisch, M. D. Kuz'min, M. Richter, *J. Magn. Magn. Mater.* **2008**, 320, 2252.
- [88] A. Fujita, S. Fujieda, Y. Hasegawa, K. Fukamichi, *Phys. Rev. B* **2001**, 65, 014410.
- [89] J. Lyubina, K. Nenkov, L. Schultz, O. Gutfleisch, *Phys. Rev. Lett.* **2008**, 101, 177203.
- [90] F. X. Hu, B. G. Shen, J. R. Sun, Z. H. Cheng, *Phys. Rev. B* **2001**, 64, 012409.
- [91] J. R. Proveti, E. C. Passamani, C. Larica, A. M. Gomes, A. Y. Takeuchi, A. Massioli, *J. Phys. D: Appl. Phys.* **2005**, 38, 1531.
- [92] A. Fujita, S. Fujieda, Y. Hasegawa, K. Fukamichi, *Phys. Rev. B* **2003**, 67, 104416.
- [93] K. Mandal, O. Gutfleisch, A. Yan, A. Handstein, K.-H. Müller, *J. Magn. Magn. Mater.* **2005**, 290, 673.
- [94] F. W. Wang, G. J. Wang, F. X. Hu, A. Kurbakov, B. G. Shen, Z. H. Cheng, *J. Phys.: Condens. Matter* **2003**, 15, 5269.
- [95] F. X. Hu, J. Gao, X. L. Qian, M. Ilyn, A. M. Tishin, J. R. Sun, B. G. Shen, *J. Appl. Phys.* **2005**, 97, 10M303.
- [96] J. Lyubina, R. Schäfer, N. Martin, L. Schultz, O. Gutfleisch, *Adv. Mater.* **2010**, 22, 3735.
- [97] L. Pytlik, A. Zieba, *J. Magn. Magn. Mat.* **1985**, 51, 199.
- [98] H. Fjellvag, A. Kjekshus, *Acta Chem. Scand., Ser. A* **1984**, 38, 719.
- [99] H. Wada, Y. Tanabe, *Appl. Phys. Lett.* **2001**, 79, 3302.
- [100] H. Wada, T. Asano, *J. Magn. Magn. Mater.* **2005**, 290, 703.
- [101] H. Wada, C. Funaba, T. Asano, M. Ilyn, A. M. Tishin, *Sci. Tech. Froid C. R., 2005* **2005**, 2005–4, 37.
- [102] N. K. Sun, W. B. Cui, D. Li, D. Y. Geng, F. Yang, Z. D. Zhang, *Appl. Phys. Lett.* **2008**, 92, 072504.
- [103] O. Hezcko, N. Scheerbaum, O. Gutfleisch, in *Nanoscale magnetic materials and applications*, (Eds: J. P. Liu, O. Gutfleisch, E. Fullerton, D. Sellmyer), Springer, New York **2009**, p. 399.
- [104] P. J. Webster, K. R. A. Ziebeck, S. L. Town, M. S. Peak, *Philos. Mag. B* **1984**, 49, 295.
- [105] F. X. Hu, B. G. Shen, J. R. Sun, G. H. Wu, *Phys. Rev. B* **2001**, 64, 132412.
- [106] J. Marcos, A. Planes, L. Manosa, F. Casanova, X. Batlle, A. Labarta, B. Martinez, *Phys. Rev. B* **2002**, 66, 224413.
- [107] Y. K. Kuo, K. M. Sivakumar, H. C. Chen, J. H. Su, C. S. Lue, *Phys. Rev. B* **2005**, 72, 054116.
- [108] W. B. Cui, W. Liu, X. H. Liu, S. Guo, Z. Han, X. G. Zhao, Z. D. Zhang, *J. Alloys Compd.* **2009**, 479, 189.
- [109] Y. Long, Z. Y. Zhang, D. Wen, G. H. Wu, R. C. Ye, Y. Q. Chang, F. R. Wan, *J. Appl. Phys.* **2005**, 98, 033515.
- [110] T. Krenke, E. Duman, M. Acet, E. F. Wassermann, X. Moya, L. Manosa, A. Planes, *Nat. Mater.* **2005**, 4, 450.
- [111] T. Krenke, M. Acet, E. F. Wassermann, X. Moya, L. Manosa, A. Planes, *Phys. Rev. B* **2005**, 72, 014412.
- [112] A. K. Pathak, I. Dubenko, J. C. Mabon, S. Stadler, N. Ali, *J. Phys. D: Appl. Phys.* **2009**, 42, 045004.
- [113] P. J. Shamberger, F. S. Ohuchi, *Phys. Rev. B* **2009**, 79, 144407.
- [114] L. Manosa, X. Moya, A. Planes, O. Gutfleisch, J. Lyubina, M. Barrio, J.-L. Tamarit, S. Aksoy, T. Krenke, M. Acet, *Appl. Phys. Lett.* **2008**, 92, 012515.
- [115] N. Scheerbaum, D. Hinz, O. Gutfleisch, K.-H. Müller, L. Schultz, *Acta Mater.* **2007**, 55, 2707.
- [116] J. Liu, N. Scheerbaum, S. Weiß, O. Gutfleisch, *Appl. Phys. Lett.* **2009**, 95, 152503.
- [117] H. Fujii, T. Hokabe, T. Komigaichi, T. Okamoto, *J. Phys. Soc. Jpn.* **1977**, 43, 41.
- [118] P. Jernberg, A. Yousif, L. Hågström, *J. Solid State Chem.* **1984**, 53, 313.
- [119] O. Beckmann, L. Lundgren, in *Handbook of Magnetic Materials*; Vol. 6, (Ed. K. H. J. Buschow), Publ. North Holland, Amsterdam, **1991**, 181.
- [120] O. Tegus, E. Brück, K. H. J. Buschow, F. R. de Boer, *Nature* **2002**, 415, 150.
- [121] E. Brück, O. Tegus, X. W. Li, F. R. de Boer, K. H. J. Buschow, *Physica B* **2003**, 327, 431.
- [122] O. Tegus, E. Brück, L. Zhang, Dagula, K. H. J. Buschow, F. R. de Boer, *Physica B* **2002**, 319, 174.
- [123] V. K. Pecharsky, K. A. Gschneider, A. O. Pecharsky, A. M. Tishin, *Phys. Rev. B* **2001**, 6414, 144406.
- [124] W. Dagula, O. Tegus, X. W. Li, L. Song, E. Brück, D. T. Cam Thanh F. R. de Boer, K. H. J. Buschow, *J. Appl. Phys.* **2006**, 99, 08Q105.
- [125] D. T. C. Thanh, E. Brück, O. Tegus, J. C. P. Klaasse, T. J. Gortenmulder, K. H. J. Buschow, *J. Appl. Phys.* **2006**, 99, 08Q107.
- [126] D. T. C. Thanh, E. Brück, N. T. Trung, J. C. P. Klaasse, K. H. J. Buschow, Z. Q. Ou, O. Tegus, L. Caron, *J. Appl. Phys.* **2008**, 103, 07B318.
- [127] A. Yan, K. H. Müller, L. Schultz, O. Gutfleisch, *J. Appl. Phys.* **2006**, 99, 08K903.
- [128] N. T. Trung, Z. Q. Ou, T. J. Gortenmulder, O. Tegus, K. H. J. Buschow, E. Brück, *Appl. Phys. Lett.* **2009**, 94, 102513.
- [129] V. K. Pecharsky, K. A. Gschneider, *J. Appl. Phys.* **2001**, 90, 4614.
- [130] M. A. Richard, A. M. Rowe, R. Chahine, *J. Appl. Phys.* **2004**, 95, 2146.
- [131] K. A. Gschneider, V. K. Pecharsky, *Int. J. Refrig.* **2008**, 31, 945.
- [132] N. T. Trung, J. C. P. Klaasse, O. Tegus, D. T. Cam Thanh, K. H. J. Buschow, E. Brück, *J. Phys. D: Appl. Phys.* **2010**, 43, 015002.
- [133] K. A. Gschneider, V. K. Pecharsky, E. Brück, H. G. M. Duijn, E. M. Levin, *Phys. Rev. Lett.* **2000**, 85, 4190.
- [134] E. Brück, M. Ilyn, A. M. Tishin, O. Tegus, *J. Magn. Magn. Mater.* **2005**, 290, 8.